Fish and Shellfish Immunology 168 (2026) 110915

Contents lists available at ScienceDirect

Fish and Shellfish Immunology

journal homepage: www.elsevier.com/locate/fsi

Full length article

# Enhancing *Edwardsiella piscicida* resistance through CRISPR/Cas9-mediated deletion of toll-like receptor 5a (*tlr5a*) in zebrafish

H.M.S.M. Wijerathna [a,b], Sumi Jung [a,c,*], Jehee Lee [a,c,**]

[a] Department of Marine Life Sciences & Center for Genomic Selection in Korean Aquaculture, Jeju National University, Jeju, 63243, Republic of Korea
[b] Department of Aquaculture and Seafood Technology, Faculty of Fisheries and Ocean Sciences, Ocean University of Sri Lanka, Colombo, 15, Sri Lanka
[c] Marine Life Research Institute, Jeju National University, Jeju, 63333, Republic of Korea

ARTICLE INFO

*Keywords:*
Toll-like receptor 5
*Danio rerio*
*Edwardsiella piscicida*
CRISPR/Cas9 gene knockout
Innate immune response

ABSTRACT

Toll-like receptor 5 (TLR5), a pattern recognition receptor that detects bacterial flagellin, plays a critical role in innate immune responses. Teleost fish possess two paralogs, *tlr5a* and *tlr5b*, of which the functional role of *tlr5a* during flagellated bacterial infections remains unclear. In this study, we investigated the involvement of *tlr5a* in the immune response against *Edwardsiella piscicida* infection in zebrafish (*Danio rerio*). To this end, we generated *tlr5a*-deficient ($tlr5a^{-/-}$) zebrafish using CRISPR/Cas9 technology. Survival analysis following *E. piscicida* challenge revealed significantly higher survival rates and reduced bacterial loads in $tlr5a^{-/-}$ larvae and adults compared to wild-type (WT) controls. $tlr5a^{-/-}$ fish exhibited significantly lower expression of pro-inflammatory cytokines (*tnfa*, *il6*, and *il-1β*), chemokine (*il8*), and pathway genes (*nfκb*, *myd88*, and *mapk14a*) at multiple time points post-infection (0, 6, 12, 24, 48, and 72 hpi). DCFH-DA staining and Sudan Black/Neutral Red staining revealed elevated reactive oxygen species (ROS) levels and immune cell recruitment, respectively, indicating reduced ROS production and diminished neutrophil and macrophage infiltration in $tlr5a^{-/-}$ larvae. Antioxidant gene expression analysis revealed reduced levels of *cat* and *nrf2* in $tlr5a^{-/-}$ larvae compared to WT. The results of this study indicate that *tlr5a* knockout attenuates excessive inflammation and improves resistance against *E. piscicida* infection, likely by reducing bacterial adhesion and suppressing NF-κB-mediated pro-inflammatory pathways. This study highlights *tlr5a* as a potential immunomodulatory target to enhance disease resistance in teleost aquaculture.

## 1. Introduction

Toll-like receptors (TLRs), central components of the innate immune system, are primary sensors capable of detecting conserved microbial motifs and triggering host defense mechanisms. Among these, Toll-like receptor 5 (TLR5) is specifically responsible for recognizing bacterial flagellin, a major structural protein of flagella, and initiating an inflammatory signaling cascade [1]. Zebrafish (*Danio rerio*) express two distinct paralogs of TLR5, namely *tlr5a* and *tlr5b*. In mammals, TLR5 functions as a homodimer; in contrast, zebrafish require the formation of a heterodimeric complex between TLR5a and TLR5b to activate the TLR5 signaling pathway. This interaction is critical for the recognition of bacterial flagellin and the subsequent activation of nuclear factor kappa-light-chain-enhancer of activated B cells (NF-κB) [2]. Both TLR5a and TLR5b receptors are type I transmembrane proteins with an extracellular domain composed of leucine-rich repeats (LRRs) for ligand recognition, a transmembrane region, and an intracellular Toll/interleukin-1 receptor (TIR) domain that is essential for triggering downstream signaling pathways [2,3]. Following engagement with bacterial flagellin, TLR5a and TLR5b activate transcription factors, such as NF-κB and activator protein-1 (AP-1), inducing the production of pro-inflammatory cytokines and chemokines that mobilize innate immune responses [4,5]. Furthermore, the recognition of bacteria by TLRs is intricately linked to the regulation of oxidative stress pathways. Pathogen detection prompts innate immune cells to produce reactive oxygen species (ROS), which serve a dual function: directly eliminating bacteria and acting as signaling mediators that amplify inflammatory responses. However, excessive ROS generation can damage host tissues, necessitating the activation of antioxidant defense mechanisms to reestablish redox homeostasis.

* Corresponding author. Marine Molecular Genetics Lab, Jeju National University, 102 Jejudaehakno, Jeju, 63243, Republic of Korea.
** Corresponding author. Marine Molecular Genetics Lab, Jeju National University, 102 Jejudaehakno, Jeju, 63243, Republic of Korea.
*E-mail addresses:* tnal1004u@jejunu.ac.kr (S. Jung), jehee@jejunu.ac.kr (J. Lee).

https://doi.org/10.1016/j.fsi.2025.110915
Received 30 July 2025; Received in revised form 5 October 2025; Accepted 6 October 2025
Available online 9 October 2025

Recent research involving teleost and mammals demonstrates that TLR5 signaling modulates oxidative stress by influencing ROS production and regulating the expression of antioxidant genes during bacterial infection [6,7]. Moreover, beyond bacterial sensing, emerging evidence indicates that teleost TLR5 paralogs have also evolved the ability to recognize viral double-stranded RNA (dsRNA) [8]. While the protective role of TLR5a has been well characterized in mammals, its specific functions in teleosts—particularly regarding pathogenic infections—remain to be fully clarified.

Recent studies indicate that flagellated bacteria exploit TLR5-mediated mechanisms to trigger immune responses and, paradoxically, facilitate bacterial adhesion and invasion into host cells [9–11]. This dual function of TLR5a has prompted further investigation into how altering this receptor impacts bacterial infections in fish. In particular, the teleost-specific properties of TLR5a are considered potential targets for genetic enhancement to improve disease resistance in aquaculture.

*Edwardsiella piscicida* is a Gram-negative bacterium that poses a significant health challenge to the aquaculture industry. *E. piscicida* is associated with various pathological conditions in fish, including hemorrhagic septicemia, septicemia, and systemic infections, which result in significant economic losses across freshwater and marine farming systems [12–15]. The bacterium's virulence is mediated by several factors, including adhesins, toxins, and specialized secretion systems [16]. Therefore, a comprehensive understanding of the interactions between *E. piscicida* and host immune factors is essential for devising effective disease management strategies.

To bolster the innate immune defenses of farmed fish, modern genetic engineering techniques have been increasingly applied in aquaculture. For example, CRISPR/Cas9-mediated genome editing is a precise and efficient method for modifying genes associated with pathogen susceptibility [17,18].

The zebrafish model offers unique advantages for genetic studies of this nature. With rapid external development, high fecundity, and transparent embryos that allow for the direct visualization of developmental processes and infection dynamics, zebrafish have become an invaluable tool for *in vivo* investigations of gene function and immune responses [19,20]. In addition, the genetic homology shared between zebrafish and humans, with over 70 % of zebrafish genes exhibiting similarity to human orthologs [21], underscores the utility of this model for translational research into immune mechanisms and disease control.

This study aimed to elucidate the role of *tlr5a* in the immune defense against *E. piscicida* infection in zebrafish. By employing CRISPR/Cas9 technology to generate *tlr5a*-deficient zebrafish, we determined how the absence of this receptor influences host survival, bacterial load, cytokine and chemokine expression profiles, reactive oxygen species (ROS) production, and the recruitment of immune cells, such as neutrophils and macrophages. The findings of this study provide novel insights into the dual functions of TLR5a in mediating host inflammatory responses and facilitating bacterial pathogenesis, thereby identifying novel targets for genetic intervention to enhance disease resistance in aquaculture.

## 2. Materials and methods

### 2.1. Zebrafish maintenance

Zebrafish were maintained as previously described [22]. The wild-type (WT) strain was used in all experimental procedures. Adult and juvenile zebrafish were raised in a water recirculating system at a constant temperature of 28 ± 0.5 °C, under a 14:10 h light-dark cycle. Embryos were maintained in embryo medium in an incubator at 28 ± 0.5 °C until the larvae hatched. The experimental protocol was approved by Jeju National University's Animal Experiment Ethics Committee (Approval number: 2019–0014).

### 2.2. In silico analysis of tlr5a

The complete coding sequence of *tlr5a* was retrieved from the Ensembl database [23], while protein sequences for related orthologs were obtained from the National Center for Biotechnology Information (NCBI) GenBank database [24]. Multiple and pairwise sequence alignments were performed using Clustal Omega Multiple Sequence Alignment tool [25] and EMBOSS Needle [26] tools, respectively, to facilitate comparative analysis. A phylogenetic tree was constructed using MEGA version 11, employing the neighbor-joining method with 5000 bootstrap replicates to ensure statistical reliability [27].

### 2.3. Generation of tlr5a knockout zebrafish using CRISPR/Cas9 technology

The *tlr5a* knockout zebrafish (*tlr5a*$^{-/-}$) was generated using the CRISPR/Cas9 gene editing tool [28]. The specific target site was identified using the Integrated DNA Technologies (IDT) (CRISPR-Cas9 guide RNA design checker | IDT (idtdna.com)). Synthesis of the target-specific single guide RNA (sgRNA) was conducted using oligonucleotides (Table 1) as previously described [29]. A mixture containing Cas9 protein (100 ng/μL) and sgRNA (50 ng/μL) was microinjected into single-cell stage embryos using a PicoPump micro-injector (World Precision Instruments, Sarasota, FL, USA). After 24 h, the efficiency of mutagenesis was evaluated via T7 Endonuclease I (T7E1; NEB, Ipswich, MA, USA) digestion as previously described [30].

F0 adult zebrafish were crossed with WT fish, and the resulting embryos were genotyped using PCR and sequence analysis to identify embryos with mutations for the F1 generation. Sequence data indicated a frameshift mutation in *tlr5a*, which was selected as the candidate mutation. The F2 generation was produced from F1 × F1 adult crosses, and genotyping was performed to identify fish with homozygous mutations in *tlr5a*. F2 fish with homozygous *tlr5a*$^{-/-}$ mutations were selected, and crosses between *tlr5a*$^{-/-}$ individuals were performed to produce further *tlr5a*$^{-/-}$ individuals for subsequent experiments. The target region was amplified using the primers listed in Table 1. For genotyping, genomic DNA was extracted from embryos, larvae, or the caudal fin tissue of adult zebrafish and used as a template for a PCR-based heteroduplex mobility assay.

### 2.4. Tissue collection, total RNA extraction, and quantitative reverse transcription PCR (RT-qPCR)

To investigate the temporal expression patterns of *tlr5a* mRNA at various developmental stages (2-cell, shield, bud, 3–4 somite stage (ss), 10 ss, 18 ss, 24 hpf, 36 hpf, 48 hpf, 3 dpf, 5 dpf, and 7 dpf), five embryos or larvae from each stage were collected, and the tissue distribution of *tlr5a* mRNA expression was analyzed. Five healthy, six-month-old zebrafish were anesthetized with 0.1 mg/mL (final concentration) tricaine methane sulfonate (MS-222; Tricaine, Sigma Aldrich, St. Louis, MO, USA). Tissues, including muscle, skin, intestine, brain, heart, testis, liver, ovary, gill, kidney, and spleen, were isolated, immediately flash frozen in liquid nitrogen, and stored at −80 °C until RNA extraction. Total RNA isolation, cDNA synthesis, and RT-qPCR were performed according to established protocols [31]. Expression of *β-actin* served as the internal control. The primers used are listed in Table 2.

### 2.5. Selection of housekeeping genes

The selection of housekeeping genes was based on their specific expression stability under different experimental conditions. Using an unsuitable reference gene can lead to inaccurate data and misinterpretation of target gene expression levels [32,33]. The most reliable reference genes were found through preliminary testing and trials. Commonly used housekeeping genes may be affected by target genes, tissues, developmental stages, treatments, or stress conditions [32,33].

**Table 1**
Oligo sequence for CRISPR/Cas9-mediated tlr5a knockout.

| Application | | Primer sequence (5′to 3′) |
|---|---|---|
| sgRNA synthesis | T7-sgRNA (Forward) | GAAATTAATACGACTCACTATACACCACCTGCGAATAGATGCgtttTagagctagaaatagcaagttAaaat |
| | Universal reverse primer | gatccgcaccgactcggtgccacttttcaagtTgataaCggactagccttatttTaacttgctatttctag |
| T7E1 assay | F | CCGGCGCAATTCATTCATGAGG |
| | R | TGAGTGAGAGTGAGATTTTTAAGGTCG |
| Mutation confirmation (RT-qPCR) | F | CTGCGAATAGATGCAGGAGC |
| | R | GTTGGACTCTCCGAATGTTGTTACG |

**Table 2**
qPCR primers used in the study.

| Gene | | Sequence (5′-3′) |
|---|---|---|
| *Tlr5a* | F | TGTGTTCAACTGATGGCTACTTCGC |
| | R | AGTCAGATCCAGCACATGAAATCGC |
| *actb* | F | CTTCCTGGGTATGGAATCTTGCGGTATC |
| | R | GGTGGAAGGAGCAAGAGAGGTGATTT |
| *ef1a* | F | CTCCTCTTGGTCGCTTTGCT |
| | R | CCGATTTTCTTCTCAACGCTCT |
| *tnfa* | F | CTCTCCGCTCTTCAGTTGACC |
| | R | GTGTGGTTTTGCCGTGGTC |
| *il6* | F | GATGAGGAGTACTTGCCGGG |
| | R | CCTGAGCCTAAATCCATGATCGC |
| *il1b* | F | TGGACTTCGCAGCACAAAATG |
| | R | GTTCACTTCACGCTCTTGGATG |
| *il8* | F | ACCTTGATGACAACTGGACAGGAGAT |
| | R | GGTGATCCGGGCATTCATGGTTT |
| *nfkb* | F | GCCGTGTCAATAGAAACTCCGGC |
| | R | CCCACGAGTCCAGGAAGAAGC |
| *myd88* | F | ACTAAGTTTGCGCTCAGTCTTTGCC |
| | R | CGCAGAATGCTGGGAAACGG |
| *mapk14a* | F | CCGTGCAGTATCAGAACTTGTCTCC |
| | R | TGGCATGGATGATGGACTGAAATGG |
| *cat* | F | CTCAGGTGCTAAATGAAGCCGAGAGA |
| | R | AGAGCCTGAACTCGGTTGCCATAA |
| *nrf2* | F | CAGTGCCTCAACATGCCAATGC |
| | R | CAGGAGGACACACTTCTGTTTGAGC |
| *gyrB1* (*E. piscicida*) | F | GCATGGAGACCTTCAGCAAT |
| | R | GCGGAGATTTTGCTCTTCTT |

β-actin (*actb1*) was chosen to normalize *tlr5a* expression in uninfected adult zebrafish. Elongation Factor 1-Alpha (*ef1a*) was used for pro-inflammatory cytokines in larvae and adults after bacterial infection or lipopolysaccharide (LPS) treatment, as well as for ROS-related genes (catalase (*cat*), nuclear factor-erythroid 2-related factor 2 (*nrf2*)), due to its stable expression during infection and stress [34]. Additionally, Glyceraldehyde-3-phosphate dehydrogenase (*gapd*) was specifically used to normalize bacterial DNA gyrase subunit B (*gyrB1*) expression. This approach, established through repeated testing, provides accurate normalization and reliable quantification. It also minimizes potential bias associated with relying on a single reference gene across multiple experimental conditions, ensuring that data reflects true biological changes rather than variations in housekeeping gene expression.

### 2.6. *E. piscicida* stock solution preparation

*E. piscicida* (ET16001, isolated from farmed olive flounder in Jeju) was first cultured in Luria-Bertani (LB) broth at 28 °C overnight until the absorbance value at $OD_{600nm}$ reached 1.3, corresponding to $6 \times 10^9$ colony-forming units (CFU)/mL (previously calculated). Subsequently, the bacterial culture was centrifuged at 3000 rpm for 30 min at 4 °C. The supernatant culture medium was removed, and the resulting pellet was washed with 1 × PBS and resuspended in 1 × PBS to generate a stock solution. Dilutions were made from the stock solution to achieve the desired concentrations for the bacterial challenge process.

### 2.7. *In vivo* survival comparison of *tlr5a*$^{-/-}$ and WT zebrafish larvae or adult fish during *E. piscicida* infection

In the larvae survival assay, 3dpf *tlr5a*$^{-/-}$ or WT larvae were divided into three groups: control (PBS-treated), $1 \times 10^7$ CFU/mL *E. piscicida* (group A), and $1 \times 10^8$ CFU/mL *E. piscicida* (group B) (n = 200 per group). Additionally, nine larvae were added to groups A and B for DNA extraction to confirm the presence of bacterial infection. Bacterial infection was conducted using an immersion technique as previously described, with some modifications [35]. 3dpf WT or *tlr5a*$^{-/-}$ group A and B larvae were immersed in $1 \times 10^7$ CFU/mL and $1 \times 10^8$ CFU/mL *E. piscicida* solution, respectively. The control group was immersed in PBS, using the same PBS concentration as that used in bacterial immersion. Larvae were kept immersed for 5 h at 28 °C, then washed three times and transferred to fresh egg water. Infected larvae were monitored for signs of mortality for approximately 10 days. Additionally, nine larvae were collected 6 h after the completion of the immersion process, and three were pooled for DNA extraction. PCR was performed using DNA gyrase subunit B (*gyrB1*) primer (Table 2) to detect *E. piscicida* infection.

In the adult challenge experiment, three-months-old adult *tlr5a*$^{-/-}$ or WT zebrafish were allocated into three groups: the control group (treated with PBS), Group A (exposed to $1 \times 10^7$ CFU/mL of *E. piscicida*), and Group B (exposed to $1 \times 10^8$ CFU/mL of *E. piscicida*) (n = 15 per group). Additionally, five fish were included in each group to confirm the presence of *E. piscicida* infection. The immersion technique was used for bacterial infection, as previously described [35]. To facilitate the infection, a wound was created near the caudal peduncle by removing 10 scales in all groups, including the control group. Adult WT or *tlr5a*$^{-/-}$ group A and B fish were exposed to $1 \times 10^7$ CFU/mL and $1 \times 10^8$ CFU/mL of *E. piscicida*, respectively. The control group was immersed in PBS with the same concentration used for bacterial immersion. The fish were kept immersed for 5 h at 28 °C, washed three times, and returned to fresh egg water. Infected fish were monitored for signs of mortality for approximately 10 days. Additionally, five fish were collected 6 h after the completion of the immersion process, and DNA was extracted for PCR analysis using *gyrB1* primers (Table 2) to confirm *E. piscicida* infection.

### 2.8. *In vivo E. piscicida* challenge assay for gene expression analysis in larvae and adult fish

For the larvae challenge experiment, WT or *tlr5a*$^{-/-}$ larvae were divided into 12 groups, with two groups for each time point for both PBS treatment and *E. piscicida* immersion (0, 6, 12, 24, 48, and 72 h). Fifteen larvae were added to each group, and the *E. piscicida* immersion process was conducted similarly to the survival assay with only $1 \times 10^7$ CFU/mL of *E. piscicida*. Following immersion, the larvae were harvested at 0, 6, 12, 24, 48, and 72 h. The collected samples were frozen at −80 °C for subsequent RNA extraction.

In the adult challenge assay, three-month-old WT or *tlr5a*$^{-/-}$ zebrafish were divided into 10 groups, with two groups for each time point for both PBS treatment and *E. piscicida* immersion (0, 6, 24, 48, and 72 h). The immersion process was conducted as performed in the adult *in vivo* survival assay using only $1 \times 10^7$ CFU/mL of *E. piscicida*.

Subsequently, internal organs and skin samples from each fish in the respective group were harvested, pooled, and flash-frozen in liquid nitrogen and stored at −80 °C for subsequent RNA extraction.

Following RNA extraction and cDNA synthesis from both larvae and adult samples, RT-qPCR analysis was performed to determine the expression levels of pro-inflammatory cytokines, chemokines, and some downstream genes of the NF-κB and MAPK pathway (*tnfa*, *il6*, *il1β*, *il8*, *nfκb*, *myd88*, and *mapk14a*); *ef1a* served as the internal control. The primers used are listed in Table 2.

### 2.9. Analysis of gene expression in WT and *tlr5a*$^{-/-}$ larvae upon stimulation with LPS

Three days post-fertilization, WT or *tlr5a*$^{-/-}$ larvae were allocated into six groups (0, 6, 12, 24, 48, and 72 h) with two sets. Six groups were designated for PBS treatment, and the other six for LPS treatment (*Escherichia coli* 0111:B4) (Sigma-Aldrich, Darmstadt, Germany). Each group consisted of 10 larvae. The LPS treatment groups of WT and *tlr5a*$^{-/-}$ larvae were exposed to 100 μg/mL of LPS, while the control group was treated with PBS. Subsequently, the larvae were maintained at 28 °C, and each group was harvested at 0, 6, 12, 24, 48, and 72 h. The samples were stored at −80 °C until RNA extraction. Following RNA extraction and cDNA synthesis, RT-qPCR was conducted to evaluate the secretion of pro-inflammatory cytokines (*tnfa*, *il6*, and *il1b*); *ef1a* served as the internal control. The primers used are listed in Table 2.

### 2.10. Analysis of ROS production and antioxidant gene expression in WT and *tlr5a*$^{-/-}$ larvae upon *E. piscicida* infection

To assess ROS production and the activation of antioxidant genes in WT and *tlr5a*$^{-/-}$ larvae, 3 dpf larvae were immersed in $1 \times 10^7$ CFU/mL of *E. piscicida* following the procedure outlined in Section 2.7. Another set of WT and *tlr5a*$^{-/-}$ larvae was treated with PBS. A group of 10 larvae was used for ROS detection, while 15 larvae in another group were used for gene expression analysis.

After 24 h of immersion, the larvae underwent DCFH-DA (Sigma-Aldrich, Germany) staining, as previously described [36]. Fluorescence images were captured using a fluorescence microscope at 400 × magnification (Leica DM6000 B; Leica Microsystem, Wetzlar, Germany). Fluorescence intensity was quantified using ImageJ version 1.54d (Wayne Rasband and contributors, National Institutes of Health, Bethesda, MD, USA). Corrected total fluorescence (CTCF) was calculated using the following formula: Integrated Density – (Area of selected cell × Mean background fluorescence). Fluorescence values are expressed in arbitrary units (a.u.), and Fluorescence intensity values were normalized to the mean of the control group and expressed as relative fold-change [37]. Another set of WT and *tlr5a*$^{-/-}$ larvae was subjected to the same *E. piscicida* infection protocol, and 24 h later, the larvae were harvested to determine the expression of antioxidant genes (*cat* and *nrf2*).

### 2.11. Evaluation of neutrophil and macrophage production in WT and *tlr5a*$^{-/-}$ larvae following *E. piscicida* infection

Three days post-fertilization, WT and *tlr5a*$^{-/-}$ zebrafish larvae (n = 10 per group) were immersed in *E. piscicida*, following the method outlined in Section 2.7. Larvae were harvested at 2, 4, and 8 hpi and fixed in 4 % paraformaldehyde overnight. Subsequently, the larvae were washed with 1 × PBST, and neutrophil staining was performed using a specific staining solution of 0.18 % Sudan black B (SIGMA-ALDRICH, St. Louis, USA). Another set of WT and *tlr5a*$^{-/-}$ larvae infected with *E. piscicida* were stained with 2.5 μg/mL of neutral red (SIGMA-ALDRICH, St. Louis, USA) for macrophage detection at 2, 4, and 8 hpi. Microscopic images were captured using an Axioskop 2 Plus microscope (Zeiss, Germany). The experimental protocol was conducted as previously described [38]. Neutrophils and macrophages were counted in each larva, and the average number of neutrophils and macrophages per larva was calculated.

### 2.12. Statistical analysis

Each experiment was performed in triplicate, and data are presented as the mean ± SD. Statistical analysis of tissue distribution was conducted using ANOVA, followed by Student's *t*-tests to assess the significance of differences between groups. Graphs were generated using the GraphPad Prism software (Version 8.0.2; GraphPad Software, Inc., San Diego, CA, USA). A *p*-value of $\leq 0.05$ was considered statistically significant.

## 3. Results and discussion

### 3.1. In silico analysis of tlr5a

Compared with the amino acid sequence of human TLR5, zebrafish Tlr5a consists of a signal peptide, leucine-rich repeats (LRR), leucine-rich repeat C-terminal (LRR_CT), transmembrane region (TM), and toll-interleukin 1-resistance (TIR) (Figs. 1 and 2) [39]. Multiple sequence analysis results reveal conserved regions, with the most highly conserved region located in the TIR domain among other orthologs (Fig. 2).

Phylogenetic tree analysis reveals that zebrafish Tlr5a is closely clustered within the fish clade (Fig. 3), and pairwise sequence comparison shows the highest identity of 76.1 % and 87.3 %, respectively, with *Ctenopharyngodon idella* (Table 3).

### 3.2. Analysis of tlr5a expression in zebrafish embryo and larval stages and various tissues in adult zebrafish

To investigate the temporal expression pattern of *tlr5a* in different developmental stages of zebrafish, embryos and larvae were collected at various time points, including the 2-cell, shield, bud, 3–4 ss, 10 ss, 18 ss, 24 hpf, 36 hpf, 4 hpf, 3 dpf, 5 dpf, and 7 dpf. Subsequently, PCR analysis was performed to assess *tlr5a* gene expression, and the resulting amplicons were visualized using agarose gel electrophoresis (Fig. 4A). The results revealed minimal *tlr5a* expression at the 2-cell stage, with a gradual increase up to 7 dpf larvae. During the initial stages, particularly at the 1-cell stage, the zygote is transcriptionally inactive, with early embryogenesis primarily regulated by maternal transcripts [40]. Activation of the embryo genome occurs at the 512-cell stage (2.75 hpf), coinciding with a gradual extension of cell cycles [41,42]. This could potentially account for the initial low expression at the 2-cell stage, followed by the gradual upregulation observed until 7dpf larvae.

Furthermore, the tissue distribution of the tlr5a transcript was analyzed in different tissues (intestine, muscle, brain, heart, kidney, gill, liver, and spleen) in healthy 6-month-old adult zebrafish. The highest expression was observed in the spleen, followed by the liver, gill, and kidney (Fig. 4B). *TLR5* is primarily expressed in epithelial and immune cells constitutively in mammals [43,44]. The spleen is a vital lymphatic organ that plays a critical role in the immune system [45], serving as a link between the innate and adaptive immune systems and facilitating an immediate response to pathogen infections [45]. Similarly, the liver is an essential organ that houses various lymphocyte populations, including natural killer and natural killer T cells, and serves as a regulator of the inflammatory process [46,47]. Liu et al. demonstrated an increase in *tlr5* expression in the gills of zebrafish after *Vibrio anguillarum* MVAV6203 bath-vaccination [48]. Previous studies have provided explanations for the underlying reasons behind the observed high expression levels of *TLR5a* in the zebrafish spleen, liver, and gills in the present study.

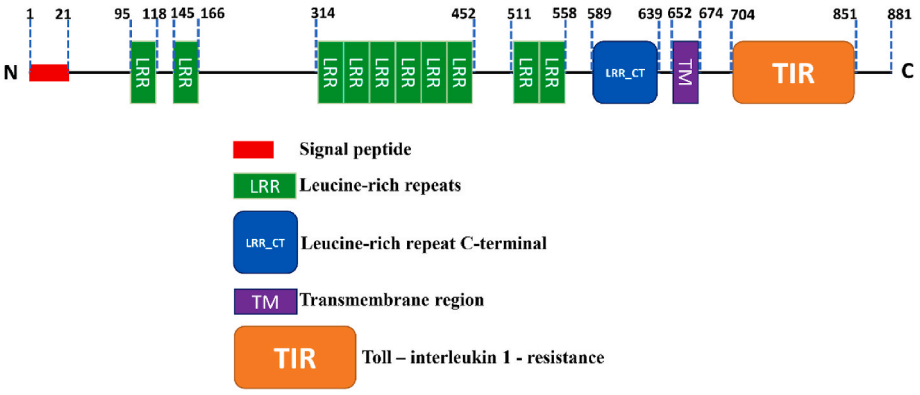


**Fig. 1.** Schematic structure of Tlr5a.

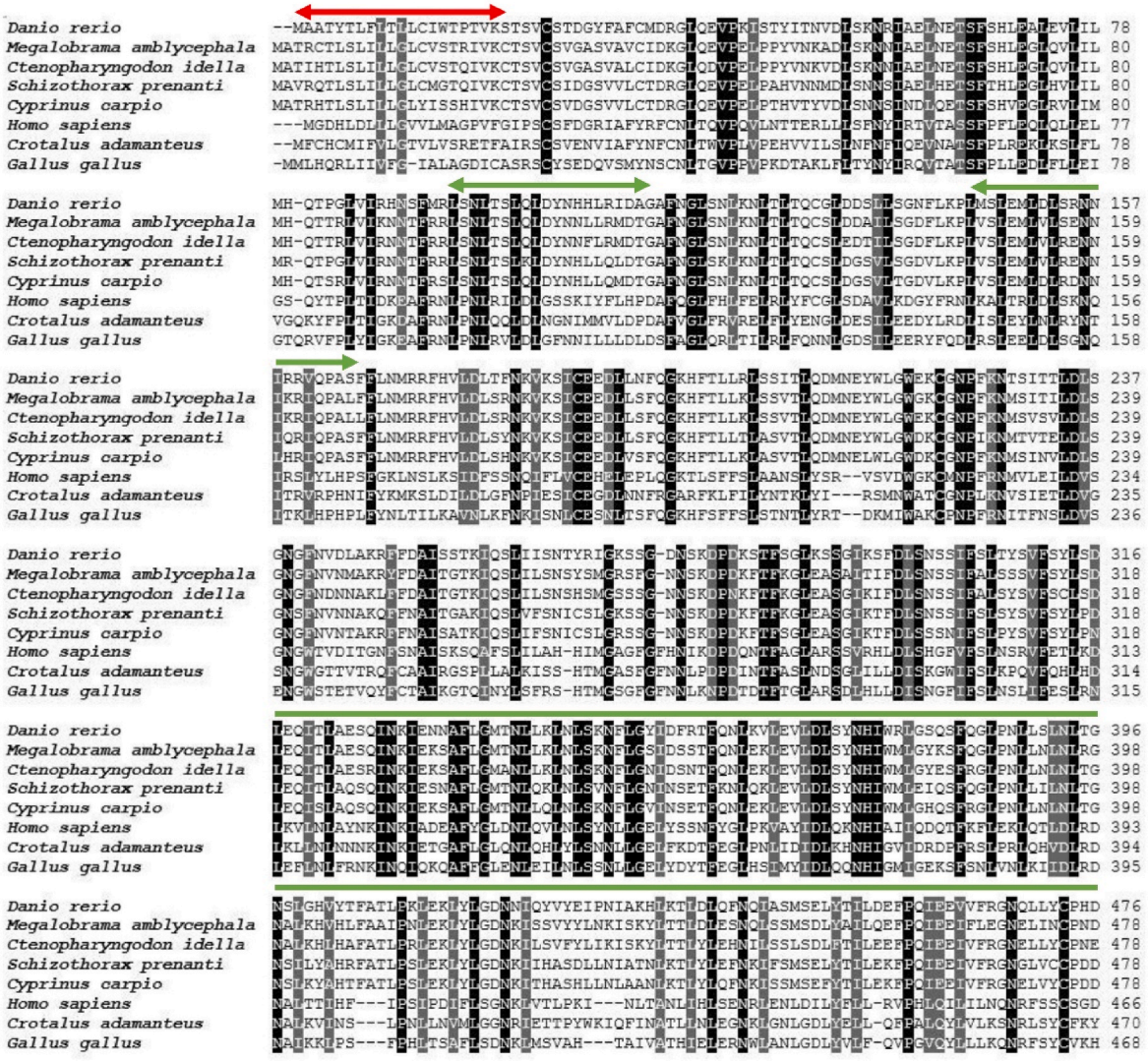


**Fig. 2.** Multiple sequence alignment of zebrafish Tlr5a with its orthologs. The Amino acids shaded in black are fully conserved, while those shaded in gray are nearly conserved.

### *3.3. Establishing a tlr5a knockout zebrafish model through CRISPR/Cas9 gene editing*

The sgRNA was designed to target a specific site within exon 2 of the zebrafish *tlr5a* gene, precisely corresponding to the 1st LRR domain (Fig. 5A). Through CRISPR/Cas9 gene editing, a 35 bp insertion was introduced at the target site, resulting in a premature stop codon (TAA) (Fig. 5B–D). This genetic alteration led to the deletion of half of the LRR1

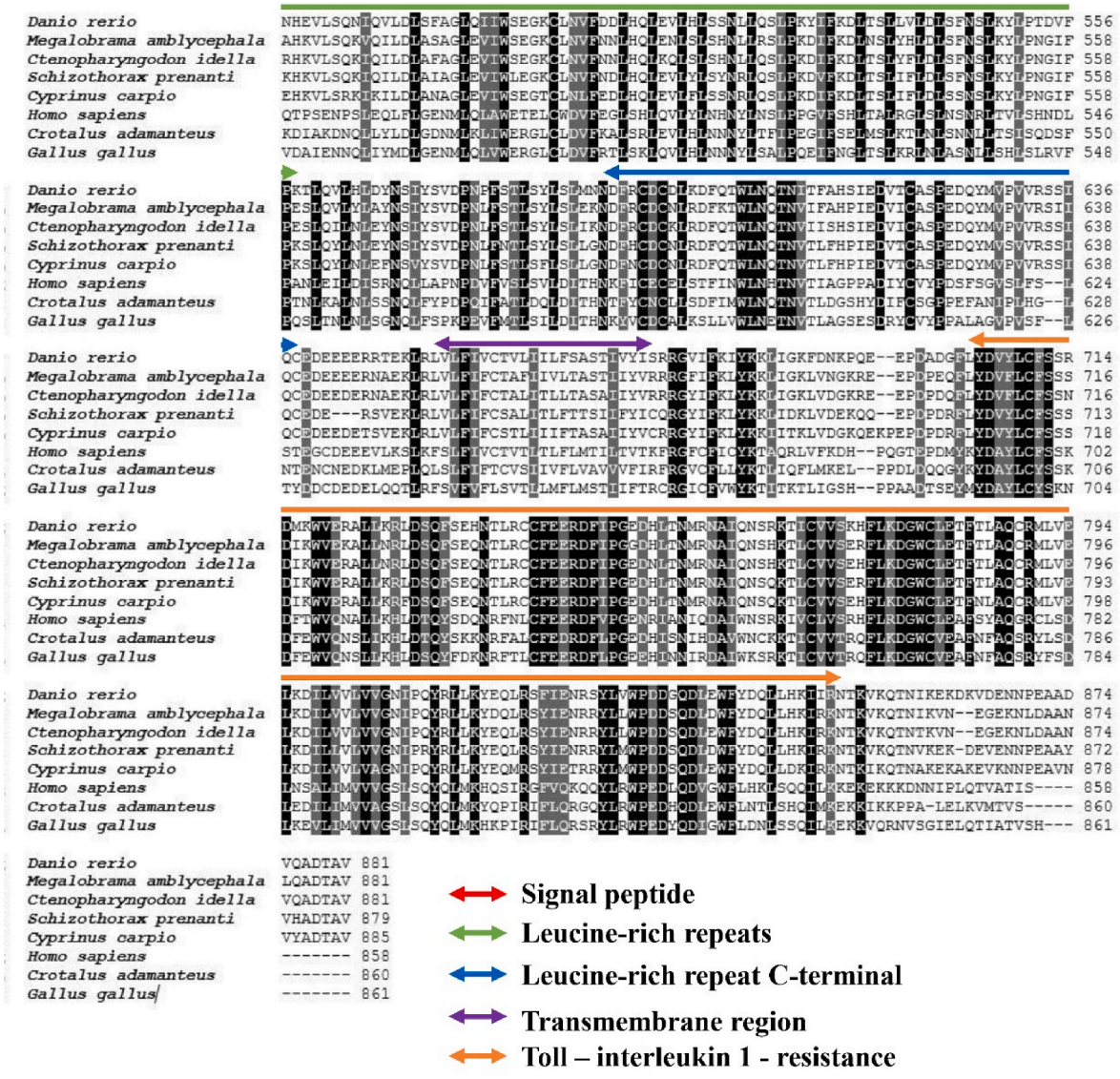


**Fig. 2.** (*continued*).

and subsequent domains, including LLR2 to 9, LRR_CT, TM, and TIR. Genotyping analysis using short primers displayed a double band in heterozygous *tlr5a* knockout fish (*tlr5a*$^{+/-}$) and a single upper band in *tlr5a* homozygous knockout larvae (*tlr5a*$^{-/-}$) (Fig. 5E). Additionally, RT-qPCR analysis revealed a complete absence of tlr5a transcription in *tlr5a*$^{-/-}$ larvae (Fig. 5F).

### 3.4. Effect of tlr5a deficiency on the attenuation of E. piscicida infection in zebrafish larvae and adult fish

To assess the impact of *tlr5a* deletion in zebrafish larvae following *E. piscicida* infection, a survival assay was conducted for 3 dpf WT and *tlr5a*$^{-/-}$ larvae (Fig. 6A and B). The larvae were exposed to *E. piscicida* at concentrations of $1 \times 10^7$ and $1 \times 10^8$ CFU/mL via immersion. Mortality was monitored over 9 days (Fig. 6B). Confirmation of *E. piscicida* infection was achieved through PCR amplification of the *gyrB1* gene of *E. piscicida* at 6 hpi, followed by agarose gel electrophoresis (Fig. 6A). The PCR results verified successful *E. piscicida* infection across all treatment groups. The lower band intensity observed in *tlr5a*$^{-/-}$ larvae than in the WT indicated reduced susceptibility to infection in *tlr5a*$^{-/-}$ larvae relative to the WT. The survival percentage graph revealed that WT larvae infected with $1 \times 10^8$ CFU/mL began to perish at 3 dpi, with the survival rate gradually declining to approximately 50 % by 9 hpi. In contrast, *tlr5a*$^{-/-}$ larvae infected with $1 \times 10^8$ CFU/mL displayed an onset of mortality at 6 hpi; however, the survival rate in *tlr5a*$^{-/-}$ larvae was higher than that of the WT. Additionally, in the case of $1 \times 10^7$ CFU/mL treatment, *tlr5a*$^{-/-}$ larvae did not exhibit any mortality even at 9 hpi, whereas WT larvae began to perish at 8 hpi, although the survival rate did not drop below 90 % even at 9 hpi.

To assess the influence of *tlr5a* absence on *E. piscicida* infection in three-month-old adult zebrafish, the survival percentage of WT and *tlr5a*$^{-/-}$ fish was evaluated following immersion with $1 \times 10^7$ and $1 \times 10^8$ CFU/mL *E. piscicida*. The efficiency of infection was confirmed by analyzing DNA extracted from adult zebrafish at 6 hpi, followed by PCR analysis for the *E. piscicida*-specific *gyrB1* gene and subsequent gel electrophoresis (Fig. 7A). Behavioral symptoms such as lethargy, reduced swimming activity, and remaining near the tank bottom or surface, as well as external signs like skin and fin hemorrhages and abdominal swelling, were analyzed in WT and *tlr5a*$^{-/-}$ fish (Fig. 7C).

The survival percentages were determined by monitoring mortality for 10 hpi (Fig. 7B). Results indicated a similar trend as observed in the larval experiment, where the WT fish displayed high-intensity bands, while the *tlr5a*$^{-/-}$ fish exhibited low-intensity bands for *gyrB1* in both *E. piscicida* concentrations (Fig. 7A). Survival percentage analysis

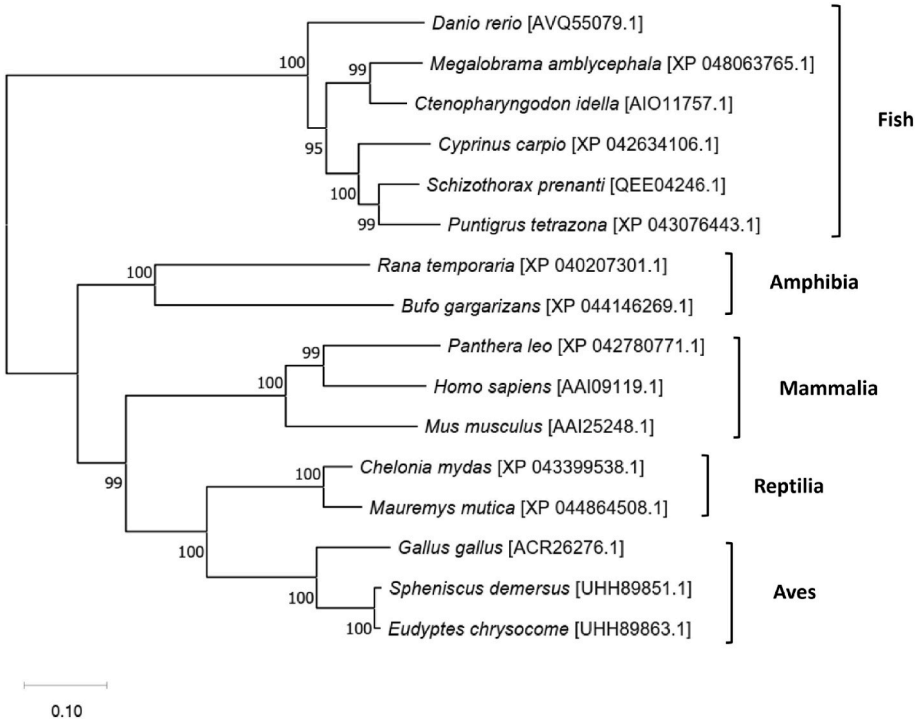


**Fig. 3.** Phylogenetic relationship of zebrafish Tlr5a with other orthologs. The Bootstrap values are indicated at the nodes of the branches based on 5000 replicates. The Neighbor-joining method was used.

**Table 3**
Comparison of pairwise percentage identity and similarity of Zebrafish Tlr5a with selected vertebrate orthologs.

| Species | Accession number | Taxonomy | Identity (%) | Similarity (%) |
|---|---|---|---|---|
| *Schizothorax prenanti* | QEE04246.1 | Fish | 75.9 | 86.3 |
| *Megalobrama amblycephala* | XP_048063765.1 | Fish | 75.9 | 86.2 |
| *Cyprinus carpio* | XP_042634106.1 | Fish | 74.9 | 86.4 |
| *Ctenopharyngodon idella* | AIO11757.1 | Fish | 76.1 | 87.3 |
| *Homo sapiens* | AAI09119.1 | Mammalia | 36.2 | 55.0 |
| *Mus musculus* | AAI25248.1 | Mammalia | 39.1 | 58.5 |
| *Rana temporaria* | XP_040207301.1 | Amphibia | 37.7 | 55.2 |
| *Bufo gargarizans* | XP_044146269.1 | Amphibia | 37.3 | 56.6 |
| *Chelonia mydas* | XP_043399538.1 | Reptilia | 38.7 | 58.4 |
| *Mauremys mutica* | XP_044864508.1 | Reptilia | 37.8 | 57.8 |
| *Gallus gallus* | ACR26276.1 | Aves | 36.2 | 55.1 |
| *Spheniscus demersus* | UHH89851.1 | Aves | 37.0 | 57.8 |

revealed that WT and *tlr5a*$^{-/-}$ fish exhibited initial mortality at 2 hpi for both concentrations (Fig. 7B). However, the survival rate was higher in *tlr5a*$^{-/-}$ fish than in WT. Moreover, fish infected with the higher concentration ($1 \times 10^8$ CFU/mL) experienced complete mortality by 4 hpi, while *tlr5a*$^{-/-}$ fish infected with the same concentration exhibited a stable but lower survival rate after 6 hpi. Similarly, WT and *tlr5a*$^{-/-}$ fish infected with the lower concentration ($1 \times 10^7$ CFU/mL) showed relatively higher survival rates in *tlr5a*$^{-/-}$ fish than the WT. Nevertheless, the overall mortality rate was higher than 50 % survival in fish infected with the lower concentration.

TLR5 is a receptor responsible for identifying flagellin bacteria and activating the innate immune system to defend against bacterial infections [2,3,49]. Scholars have also investigated the various functions of TLR5 in different organs, such as the respiratory tract, gastrointestinal tract, liver, and dorsal root ganglion neurons [50]. The intestine, a crucial organ that houses essential microbiota, may also be susceptible

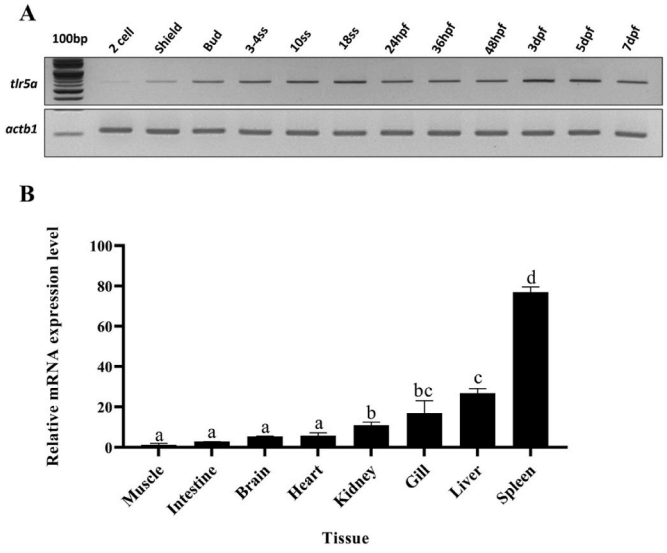


**Fig. 4.** Analysis of *tlr5a* transcript levels in different developmental stages and various tissues of adult zebrafish. **(A)** Temporal expression pattern of *tlr5a* in different developmental stages of zebrafish. PCR was conducted to analyze the expression of *tlr5a* in each stage using cDNA as a template. *actin-β1* was amplified in the same samples as an indicator for normalization. **(B)** Tissue-specific expression levels of *tlr5a* in healthy adult zebrafish were examined. The relative mRNA expression levels of *tlr5a* were evaluated in various organs, with muscle used as the reference. The spleen and liver exhibited the highest expression levels, followed by relatively elevated levels in the gills and kidneys compared to other tissues. Data were normalized to *actin-β1*. Each bar on the graph represents the mean relative mRNA expression level, with error bars indicating SD (n = 3). Statistical significance was determined using one-way ANOVA with Tukey's post hoc test. Different letters indicate statistically significant differences ($p < 0.05$) between tissue types.

to colonization by various toxigenic or opportunistic pathogenic

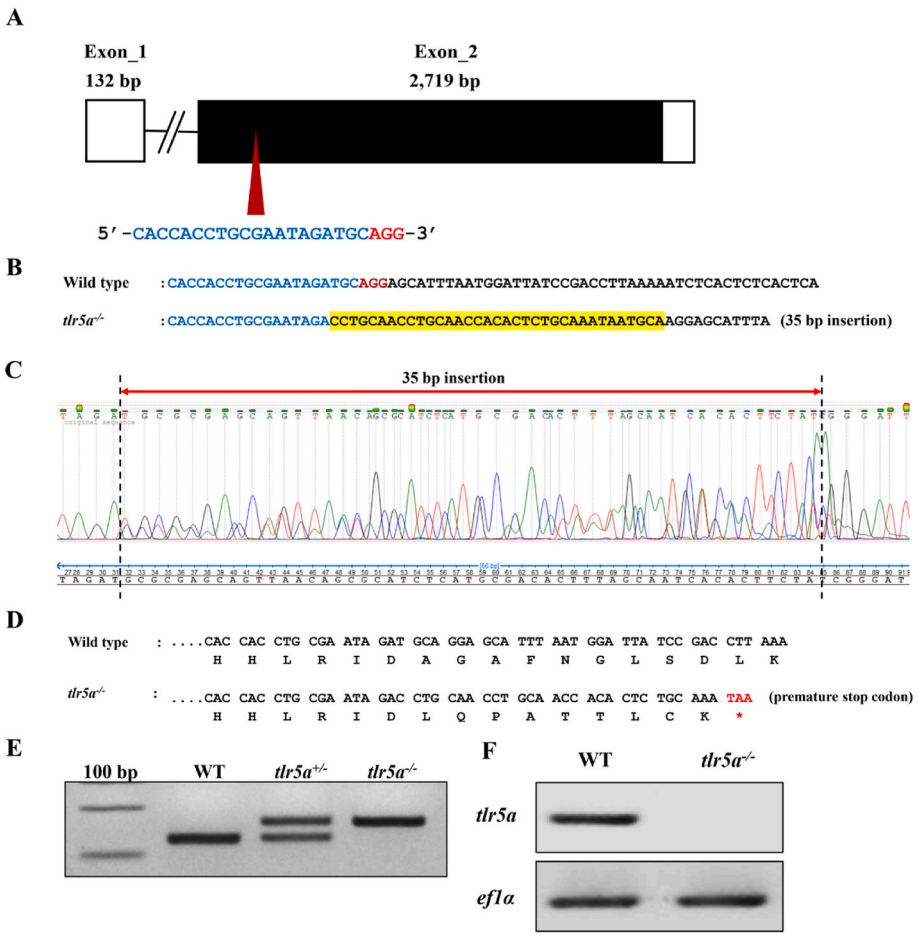


**Fig. 5.** Generation and characterization of *tlr5a*$^{-/-}$ fish. **(A)** Schematic representation of the zebrafish *tlr5a* gene organization. Untranslated regions and open reading frames are represented by white and black boxes, respectively. The sgRNA target site is indicated by the red arrowhead. The PAM and sgRNA target sequences are highlighted in red and blue letters, respectively. **(B–D)** Depiction of the 35-bp nucleotide insertion at the target site, leading to the introduction of a premature stop codon via CRISPR/Cas9 gene editing. The inserted amino acid sequence is highlighted in yellow. **(E)** Genotyping analysis of *tlr5a*$^{+/-}$ and *tlr5a*$^{-/-}$ using PCR and agarose gel electrophoresis. **(F)** Validation of the mutation through RT-qPCR analysis employing *tlr5a* target site-specific primers in 7dpf WT and *tlr5a*$^{-/-}$ larvae.

bacteria [50]. Consequently, uncontrolled activation of TLR5 can overstimulate the immune system, leading to subsequent chronic gut inflammation [51]. TLR5 senses the composition and localization of intestinal microbiota to prevent inflammatory diseases in the intestine [52]. However, TLR5 plays a crucial role in maintaining immune homeostasis and defending against bacterial infections [52]. Moreover, the liver is continually exposed to different types of bacteria, some of which are systemic and of gut origin [50]. Therefore, TLR5 may exhibit an immunosuppressive response against bacteria or bacteria-derived molecules, thereby preventing constant liver inflammation [53]. The functional role of TLR5 is complex and requires further elucidation [50].

Our results demonstrate that the absence of zebrafish *tlr5a* reduces the infection efficiency of *E. piscicida*, a flagellated bacterium (Figs. 6 and 7). Other studies have indicated that flagellin serves as a pathogen-associated molecular pattern, activating TLR5 and initiating the innate host response in mammals [1,54]. Tallant et al. have described how the expression of flagellin in flagellated bacteria (*Salmonella*) is necessary for bacterial invasion [55]. Consistent with our findings, Dai et al. have revealed that the overexpression of TLR5 in pig intestinal epithelial (IPEC-J2) cells enhances the adhesion and infection of *Escherichia coli*, a flagellated bacterium, whereas low expression of TLR5 has the opposite effect [9]. Moreover, the authors have concluded that suppressing TLR5 in piglets may enhance resistance against *E. coli* due to the reduced adhesion efficiency of *E. coli* to host cells via TLR5 [9]. This adhesion process can potentially contribute to the establishment of the infection by promoting the attachment of bacteria to host cells, enabling them to evade the host immune response and initiate colonization. Similarly, Uematsu et al. have revealed that the flagellin bacteria *S. typhimurium* internalization and subsequent infection of internal organs, such as the liver and spleen, occur through the adhesion to intestinal macrophages CD11c$^{+}$ in mice [11]. *E. tarda* has the potential to survive and replicate in host phagocytes [56]. However, the exact mechanisms and implications of this interaction may vary depending on the specific bacterial and host contexts; further research is necessary to fully understand the intricacies of this process. Taken together, the absence of *tlr5a* attenuates *E. piscicida* infection in zebrafish.

### 3.5. Analysis of pro-inflammatory cytokine, chemokine, and pathway activation in *E. piscicida*-infected *tlr5a*$^{-/-}$ and WT zebrafish

The TLR5 is crucial in detecting flagellin bacterial infections and activating innate immune defenses against such bacteria [51]. TLR5 activation triggers the induction of various chemokines, pro-inflammatory cytokines, reactive oxygen species, and anti-inflammatory cytokines through the MyD88-dependent NF-κB signaling pathway and the MAPK pathway [53,57].

Therefore, in this study, we examined the activation of chemokines (such as *il8*) and pro-inflammatory cytokines (*tnfa*, *il6*, and *il1b*), as well as the activation of the NF-κB and MAPK pathways by analyzing the mRNA expression levels of *myd88*, *nfkb*, and *mapk14a* using the RT-qPCR method following the infection of *E. piscicida* in both WT and *tlr5a*$^{-/-}$ zebrafish larvae and adults (Figs. 8 and 9).

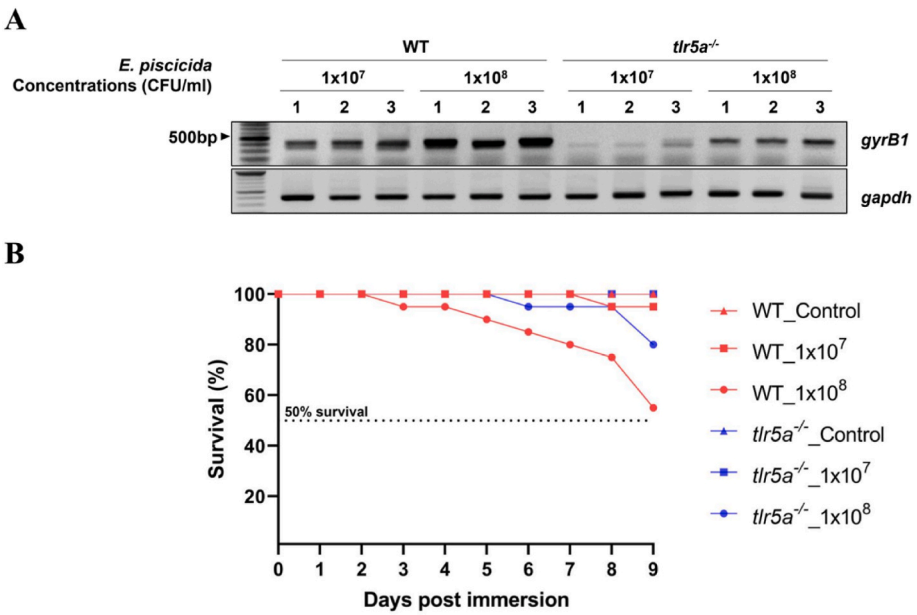


**Fig. 6.** Confirmation of *E. piscicida* infection efficiency and survival rate in WT and *tlr5a*$^{-/-}$ zebrafish larvae. Three days post-fertilization, WT and *tlr5a*$^{-/-}$ larvae were subjected to immersion with $1 \times 10^7$ and $1 \times 10^8$ CFU/mL *E. piscicida* for 5 h. **(A)** Verification of infection efficiency through PCR analysis of *E. piscicida gyrB1* gene, followed by agarose gel electrophoresis of larvae harvested at 6hpi. *gapdh* was utilized as an internal control. **(B)** Assessment of survival rates in WT and *tlr5a*$^{-/-}$ larvae following *E. piscicida* infection.

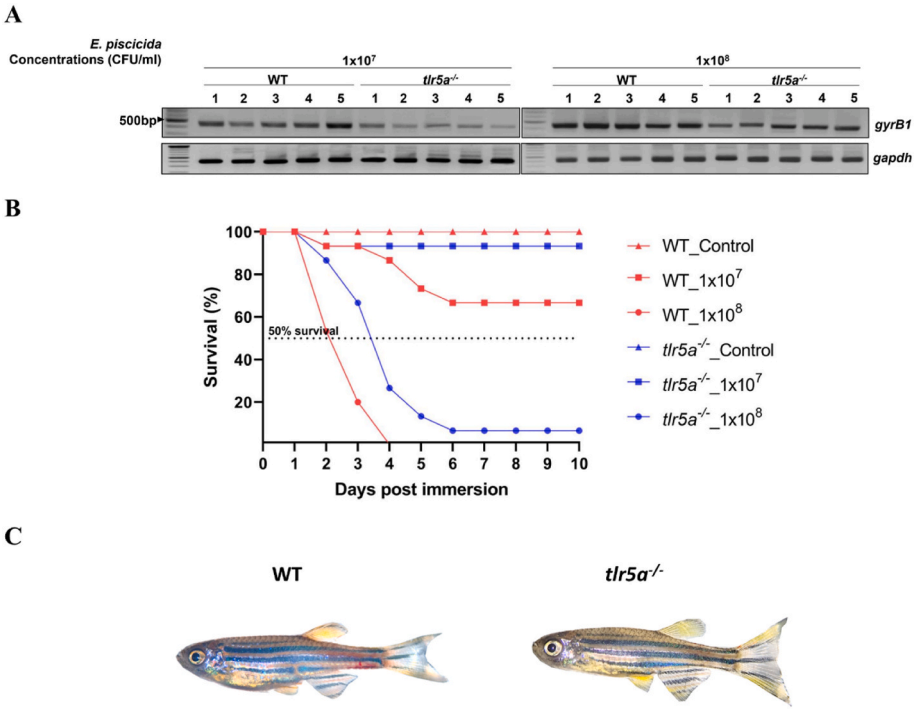


**Fig. 7.** Confirmation of *E. piscicida* infection efficiency and survival rate in WT and *tlr5a*$^{-/-}$ adult zebrafish. At six months old, WT and *tlr5a*$^{-/-}$ fish underwent immersion in $1 \times 10^7$ and $1 \times 10^8$ CFU/mL *E. piscicida* for 5 h. **(A)** The efficiency of infection was verified through PCR analysis of the *E. piscicida gyrB1* gene, followed by agarose gel electrophoresis of the harvested larvae at 6 hpi. Normalization was performed using the internal control glyceraldehyde-3-phosphate dehydrogenase (*gapdh*). **(B)** The survival rates of WT and *tlr5a*$^{-/-}$ adult fish were assessed following *E. piscicida* infection. **(C)** *E. piscicida* infected WT and *tlr5a*$^{-/-}$ zebrafish.

In the case of the larvae challenge experiment, 3 dpf WT and *tlr5a*$^{-/-}$ zebrafish larvae were infected with *E. piscicida*, and the gene expression analysis was conducted at 6, 12, 24, 48, and 72 hpi using RT-qPCR. As expected, the absence of tlr5a in *tlr5a*$^{-/-}$ zebrafish larvae reduced the activation of pro-inflammatory cytokines *tnfa*, *il6*, and *il1b*, as well as the chemokine *il8* mRNA expression levels compared to the WT larvae (Fig. 8A–D). The first significant differences in the activation of *tnfa*, *il6*, *il1b,* and *il8* were observed at 12, 24, 6, and 6 hpi, respectively, between WT and *tlr5a*$^{-/-}$ larvae (Fig. 8A–D). Moreover, *tnfa*, *il6*, *il1b,* and *il8* showed their highest expression levels at 48, 24, 72, and 72 hpi,

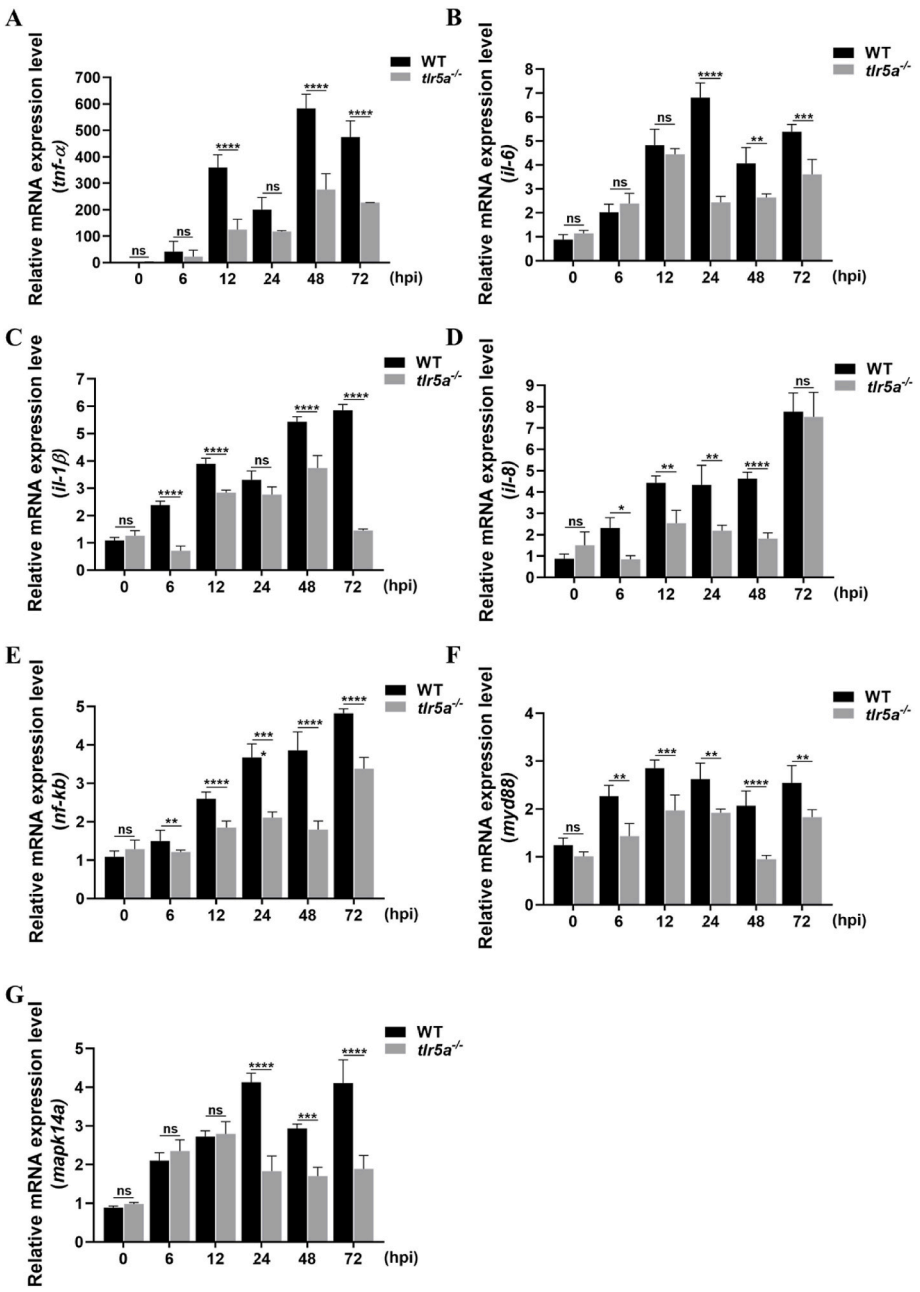


**Fig. 8.** Temporal gene expression analysis in WT and *tlr5a*$^{-/-}$ larvae upon *E. piscicida* infection. Three-day-post-fertilization, WT and *tlr5a*$^{-/-}$ zebrafish larvae were infected with $1 \times 10^7$ CFU/mL of *E. piscicida*. Pro-inflammatory cytokines (*tnfa*, *il6*, and *il1b*) **(A–C)**, chemokine (*il8*) **(D)**, and pathway gene (*nfkb*, *myd88*, and *mapk14a*) **(E–G)** activations were analyzed at 0, 6, 12, 24, 48, and 72 hpi) using the RT-qPCR method. Data were normalized to *ef1a* and the gene expression of PBS-treated groups. Each bar represents the mean relative mRNA expression level, with error bars indicating SD (n = 3). Statistical significance between the WT and *tlr5a*$^{-/-}$ larvae was determined using Student's *t*-test. ns, non-significance ($p > 0.05$); *, $p \leq 0.05$; **, $p \leq 0.01$; ***, $p \leq 0.001$; ****, $p \leq 0.0001$.

respectively. However, even though the highest expression of *il8* was observed after 72 hpi, no significant difference between WT and *tlr5a*$^{-/-}$ larvae was observed (Fig. 8D). Furthermore, NF-κB and MyD88 activation and a significant difference between WT and *tlr5a*$^{-/-}$ larvae were observed after 6 hpi (Fig. 8E and F). However, *mapk14a* activation was observed after 24 hpi (Fig. 8G).

The results of the three-month-old adult challenge experiment showed a low level of *tnfa*, *il6*, *il1b*, *il8*, *nfkb*, *myd88*, and *mapk14a* activation in *tlr5a*$^{-/-}$ fish compared to WT (Fig. 9). The highest expression of *tnfa*, *il6*, *il1b*, *il8*, *nfkb*, *myd88*, and *mapk14a* was at 24, 48, 24, 6, 24, 6, and 48 hpi, respectively. However, the expression showed an undulatory modulation pattern in both larvae and adult zebrafish (Figs. 8 and 9). The reason for this undulatory modulatory pattern of different genes is the complex mechanism of each cell signaling pathway during immune activation. This complexity arises from the number of components and isoforms that have partially overlapping functions [58]. Furthermore, each pathway exhibits a distinct temporal activation pattern specific to the pathway in response to various types of pathogen infections [59], and several pathways may be involved in controlling each molecule.

Consistent with our results, flagellin has been reported to activate NF-κB, MAPK, and pro-inflammatory gene expression via TLR5 in human colorectal adenocarcinoma cells (HT-29 cells) [55]. Dai et al. revealed that the absence of TLR5 in piglets attenuated *E. coli* infection and reduced the overactivation of inflammation and cell damage by decreasing the activation of the MyD88-dependent NF-κB pathway and

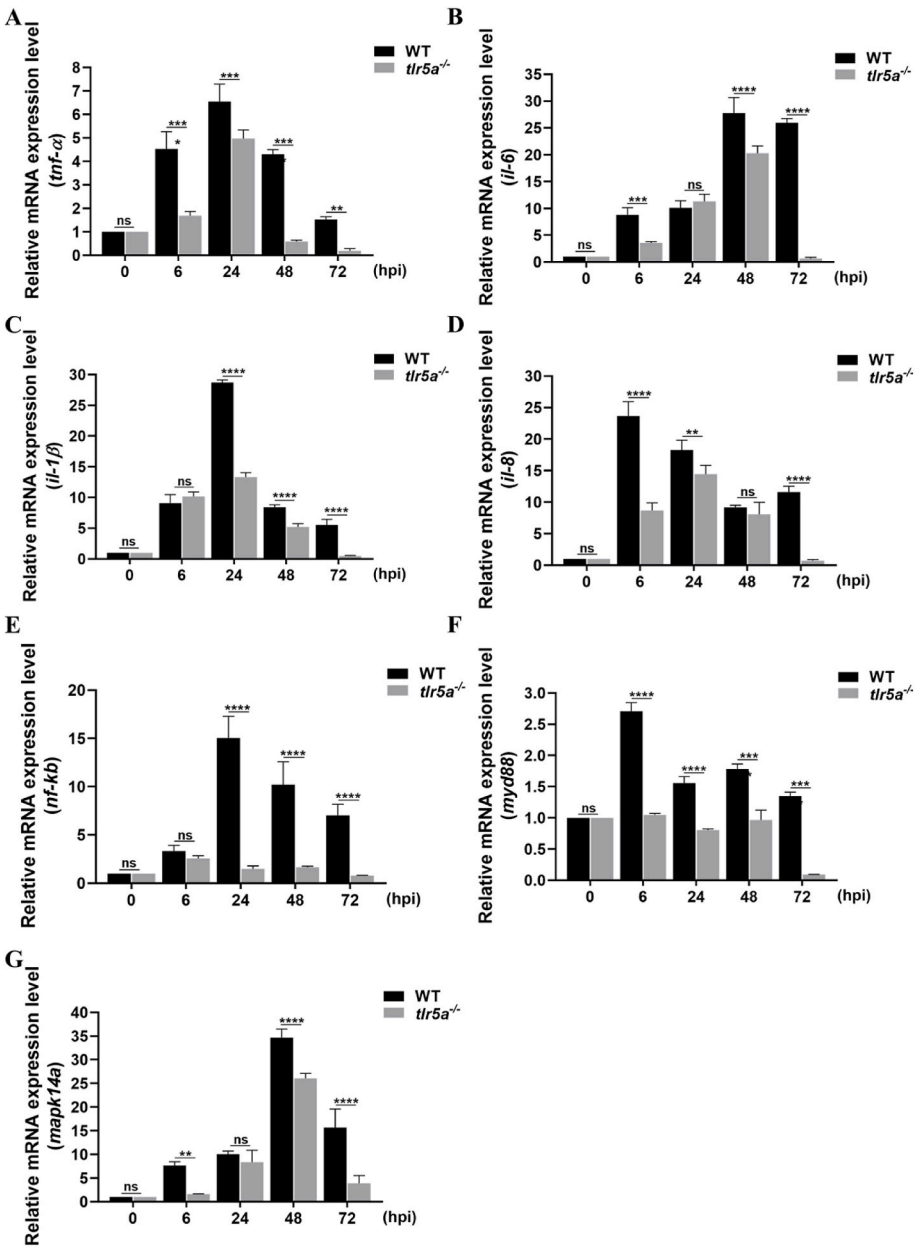


**Fig. 9.** Temporal gene expression analysis in adult WT and *tlr5a*$^{-/-}$ zebrafish upon *E. piscicida* infection. *E. piscicida* infection was initiated in three-month-old WT and *tlr5a*$^{-/-}$ zebrafish at a concentration of $1 \times 10^7$ CFU/mL. Analysis of pro-inflammatory cytokines (*tnfa*, *il6*, and *il1b*) **(A–C)**, chemokine (*il8*) **(D)**, and pathway gene (*nfkb*, *myd88*, and *mapk14a*) **(E, F, and G)** activations was conducted. RT-qPCR was utilized to measure the gene expression at specific time points post-infection, including 0, 6, 24, 48, and 72 hpi. The data were normalized to *ef1a*, and comparisons were made with the gene expressions of the PBS-treated groups. Each bar represents the mean relative mRNA expression level, while the error bars indicate the SD (n = 3). The statistical significance between the WT and *tlr5a*$^{-/-}$ fish was determined using Student's *t*-test (ns, non-significance ($p > 0.05$); *, $p \leq 0.05$; **, $p \leq 0.01$; ***, $p \leq 0.001$; ****, $p \leq 0.0001$.).

pro-inflammatory cytokines (TNF-α, IL-6, IL-8, IL-10, and IL-12).

Taken together, the absence of *tlr5a* reduces the activation of pro-inflammatory cytokines, chemokines, as well as the NF-κB and MAPK pathways upon *E. piscicida* infection, potentially attenuating excessive inflammation and cell damage.

### 3.6. Effect of tlr5a deficiency on LPS-induced pro-inflammatory cytokine activation

The temporal expression profile (0, 6, 12, 24, 48, and 72 h post-treatment [hpt]) of pro-inflammatory cytokines (*tnfa*, *il6*, and *il1b*) was analyzed in WT and *tlr5a*$^{-/-}$ larvae upon stimulation with LPS (Fig. 10). Our results showed no significant differences in pro-inflammatory cytokines between the WT and *tlr5a*$^{-/-}$ larvae at all the time points following LPS treatment. However, LPS treatment enhanced *tnfa*, *il6*, and *il1b* levels after 6 hpt, gradually decreasing thereafter until 72 hpt in WT and *tlr5a*$^{-/-}$ larvae. LPS, a component of the cell membrane of gram-negative bacteria, acts as a bacterial mimic, inducing systemic inflammation [60]. Comprising lipid A, O side chains, and a core oligosaccharide, LPS is characterized by its lipid A, which serves as the pathogen-associated molecular pattern (PAMP) of LPS [61,62]. Previous research has indicated that the TLR4/myeloid differentiation factor 2/cluster of differentiation 14 (TLR4/MD-2/CD14) complex acts as the primary receptor for LPS in mammals [63]. In contrast, zebrafish lack this mechanism; therefore, TLR4-independent pathways—including scavenger receptors (SRs), NOD1-dependent cytosolic sensing,

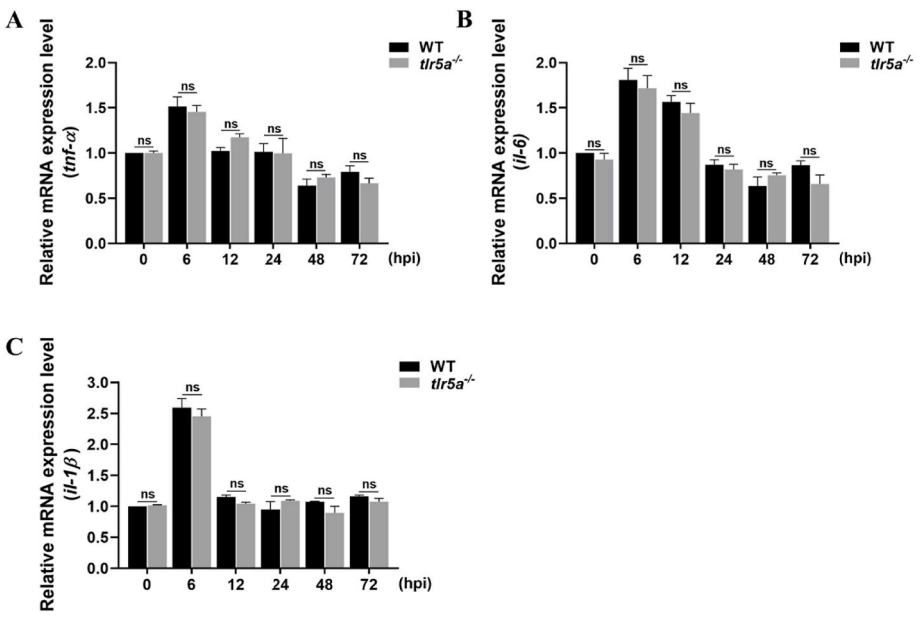


**Fig. 10.** Temporal expression profile of pro-inflammatory cytokines upon LPS treatment to WT and *tlr5a*$^{-/-}$ zebrafish larvae. Three days post-fertilization, zebrafish larvae were treated with 100 μg/mL LPS, and gene expressions of **(A)** *tnfa*, **(B)** *il6*, and **(C)** *il1b* were analyzed using RT-qPCR at 0, 6, 12, 24, 48, and 72 hpt. The data were normalized to *ef1a*, and comparisons were made with the gene expressions of the PBS-treated groups. Each bar in the graph represents the mean relative mRNA expression level, while the error bars indicate the SD (n = 3). The statistical significance between the WT and *tlr5a*$^{-/-}$ fish was determined using Student's *t*-test (ns, non-significance; $p > 0.05$).

peptidoglycan recognition proteins (PGRPs), complement component 3 (C3), and Caspase-1-like protein 2 (Caspy2)-mediated inflammasome activation—may contribute to LPS recognition in zebrafish [64].

Moreover, Previous studies have demonstrated differences in pro-inflammatory cytokine production in LPS-treated BM-derived dendritic cells from WT or TLR5 knockout mice, emphasizing the specificity of TLR5 in recognizing flagellin [65]. This finding explains the results in the present study. In conclusion, tlr5a is specific to flagellin and exhibits no sensitivity to LPS.

### 3.7. Effect of tlr5a deficiency on ROS production and antioxidant gene expression in zebrafish larvae upon E. piscicida infection and LPS treatment

ROS, critical in the early immune response against pathogen infections, are highly toxic to pathogens and are therefore utilized by the host as a defense mechanism to prevent bacterial colonization [66]. ROS can also augment the cellular response against bacterial growth and colonization by inducing apoptosis of infected cells and triggering other immune responses [67].

Herein, we examined the impact of *tlr5a* deficiency on ROS production in zebrafish larvae following *E. piscicida* infection and LPS treatment. To this end, 3dpf WT and *tlr5a*$^{-/-}$ larvae were infected with $1 \times 10^7$ CFU/mL *E. piscicida* or treated with 100 μg/mL of LPS through immersion. Control groups were treated with PBS. Subsequently, DCFH-DA staining was conducted after 24 h to measure ROS fluorescence in *E. piscicida*-infected (Fig. 11A and B) larvae, and the relative fluorescence intensity was determined using ImageJ software. Another set of WT and *tlr5a*$^{-/-}$ larvae infected with *E. piscicida* was used to assess the expression of antioxidant-related genes (*cat* and *nrf2*) after 24 h (Fig. 11C and D).

*E. piscicida* infection in WT larvae yielded higher levels of fluorescence than *tlr5a*$^{-/-}$ larvae (Fig. 11A and B), while no significant differences were observed in PBS-treated larvae. Additionally, analysis of antioxidant gene (*cat* and *nrf2*) induction upon *E. piscicida* infection revealed reduced expression levels of both genes in *tlr5a*$^{-/-}$ larvae compared to WT.

Joo et al. reported that flagellin can induce hydrogen peroxide ($H_2O_2$) production, which is crucial in the innate immune response mediated by TLR5 in nasal epithelial cells [68].

The results suggest that *tlr5a*$^{-/-}$ larvae exhibit a reduced level of ROS production upon *E. piscicida* infection, potentially attributed to the lower level of bacterial infection or the attenuation of Tlr5a-related immune signaling pathway activations.

### 3.8. Effect of E. piscicida infection to WT and tlr5a$^{-/-}$ larvae on neutrophil and macrophage production

Neutrophils, circulating leukocytes, are among the first responders of the immune system, recruited to sites of infection or injury [69]. Upon infection or injury, neutrophils migrate from hematopoietic tissues to the site via the vasculature and engage in defense mechanisms, such as phagocytosis, the secretion of antimicrobial substances, including granule proteins, the production of ROS, and the release of Neutrophil Extracellular Traps (NETs) [70,71].

The effect of *tlr5a* deficiency on triggering neutrophil production in response to *E. piscicida* infection was investigated by infecting 3 dpf WT and *tlr5a*$^{-/-}$ larvae with $1 \times 10^7$ CFU/mL *E. piscicida* via immersion. Sudan Black staining was conducted at 0, 4, 8, and 12 hpi, followed by image capture (Fig. 12A). The average number of neutrophils was subsequently counted (Fig. 12B). The results showed a higher production of neutrophils in the CHT area of WT larvae than *tlr5a*$^{-/-}$ larvae, indicating heightened stimulation likely due to increased bacterial infection.

This conclusion is supported by findings from Zhang et al., showing that two strains of *Klebsiella pneumoniae*, each with varying infection potentials, induced a higher number of neutrophils in the CHT area of zebrafish than the uninfected control group. Additionally, larvae immersed with the strain exhibiting greater infection potential displayed a higher neutrophil count than the other strain [72].

Macrophages, similar to neutrophils, are key phagocytic cells within the innate immune system [73]. They detect pathogenic invasions or tissue damage through pathogen-associated molecular patterns (PAMPs) or damage-associated molecular patterns (DAMPs), respectively, along with host-derived inflammatory mediators. Upon detection,

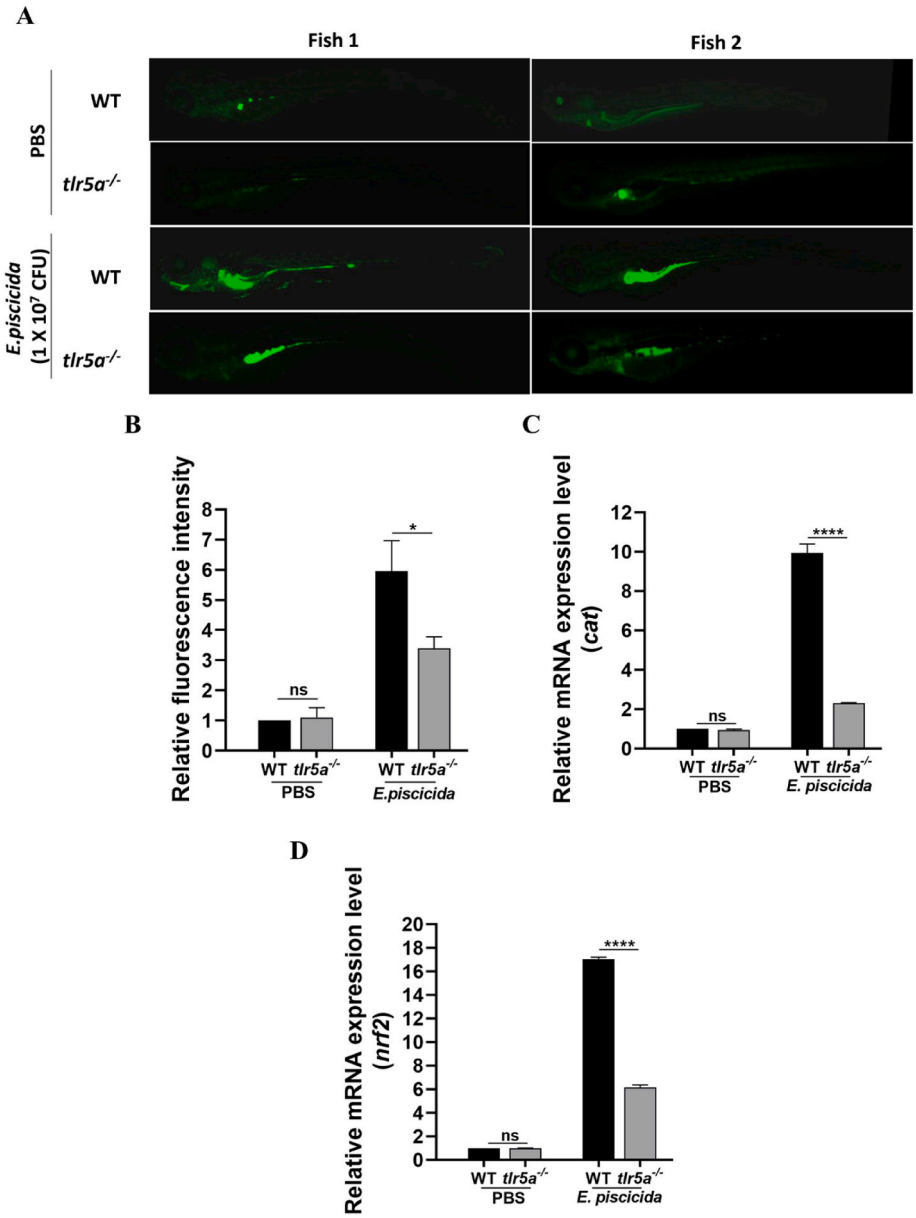


**Fig. 11.** Impact of *tlr5a* deletion on *E. piscicida*-induced ROS production and antioxidant gene expression in zebrafish larvae. Three days post-fertilization, WT and *tlr5a*$^{-/-}$ larvae were immersed in 1 × $10^7$ CFU/mL *E. piscicida*, and 24 h later, **(A)** DCFH-DA staining and fluorescence images were captured to detect ROS, while **(B)** the relative fluorescence intensity was calculated using ImageJ software. The expression of antioxidant genes **(C)** *cat* and **(D)** *nrf2* was analyzed using RT-qPCR. RT-qPCR data were normalized to *ef1a*, and comparisons were made with the gene expressions of the PBS-treated groups. Each bar represents the mean relative mRNA expression level, with error bars indicating the SD (n = 3). The statistical significance between the WT and *tlr5a*$^{-/-}$ fish was determined using Student's *t*-test (ns, non-significance ($p > 0.05$); *, $p \leq 0.05$; ****, $p \leq 0.0001$).

macrophages migrate to the site of infection to initiate the phagocytosis process [73,74] and release cytotoxic factors, chemokines, and cytokines to orchestrate the inflammatory response [75,76].

To investigate the impact of *tlr5a* deficiency in zebrafish larvae on macrophage production in response to *E. piscicida* infection, WT and *tlr5a*$^{-/-}$ larvae were immersed in 1 × $10^7$ CFU/mL *E. piscicida* and stained with neutral red staining at 0, 4, 8, and 12 hpi (Fig. 13). Consistent with the neutrophil results, reduced macrophage counts in *tlr5a*$^{-/-}$ larvae were observed compared to WT larvae. WT larvae exhibited higher neutrophil and macrophage counts compared to *tlr5a*$^{-/-}$ larvae, suggesting that Tlr5a deficiency diminishes the recruitment or production of these immune cells following bacterial challenge. These results indicate that the absence of Tlr5a may either directly compromise immune cell induction or indirectly limit bacterial invasion, thereby leading to reduced neutrophil and macrophage responses in *tlr5a*$^{-/-}$ zebrafish.

Notably, a previous study involving neutral red staining after immersion infection with two strains of *K. pneumoniae* demonstrated enhanced macrophage production, akin to the behavior observed in neutrophils, compared to uninfected control zebrafish larvae [72].

Taken together, the absence of *tlr5a* may directly affect the induction of bacterial-responsive neutrophils and macrophages, or the attenuation of *E. piscicida* infection due to the lack of *tlr5a* adhesion, resulting in lower levels of neutrophils and macrophages in infected *tlr5a*$^{-/-}$ zebrafish than WT.

## 4. Conclusion

The investigation into the impact of *tlr5a* deficiency on *E. piscicida* infection in zebrafish larvae and adult fish unveiled novel insights. The

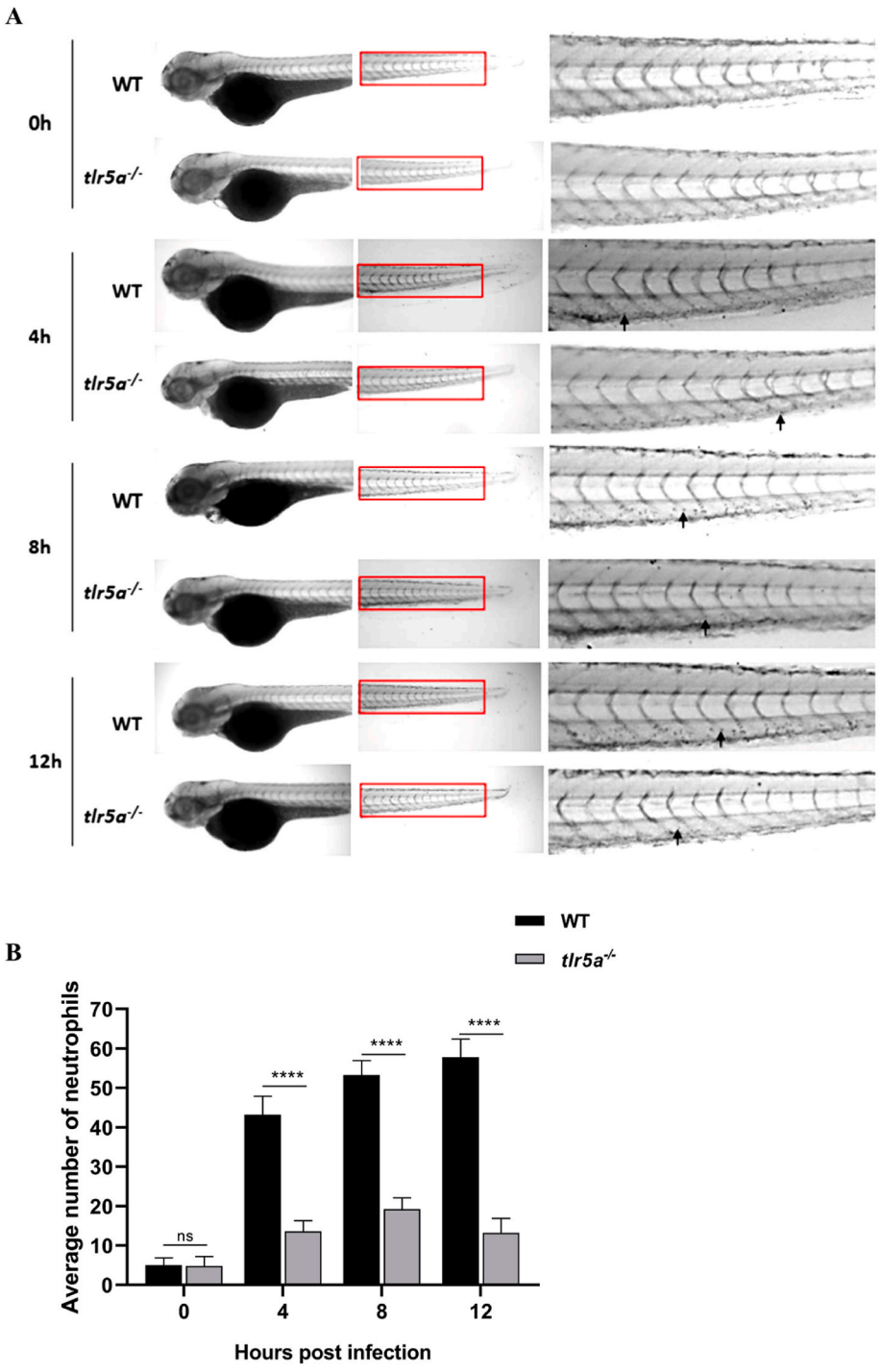


**Fig. 12.** Impact of *tlr5a* deficiency on neutrophil production upon *E. piscicida* infection. Three days post-fertilization, WT and *tlr5a*$^{-/-}$ zebrafish larvae were immersed in *E. piscicida*, followed by Sudan black staining at 0, 4, 8, and 12 hpi to visualize the neutrophils **(A)**. The average neutrophil count was obtained and graphed **(B)**. Each bar in the graphs represents the average neutrophil count, with error bars indicating the SD (n = 10). The statistical significance between the WT and *tlr5a*$^{-/-}$ fish was determined using Student's *t*-test (ns, non-significance, $p > 0.05$; ****$p \leq 0.0001$).

absence of *tlr5a* reduced infection efficiency, attenuated activation of pro-inflammatory cytokines and chemokines, and dampened NF-κB and MAPK pathway responses. A notable decrease in ROS production and lower levels of neutrophils and macrophages were also observed, suggesting a potential impairment in immune responses in *tlr5a*$^{-/-}$ zebrafish upon *E. piscicida* infection. The effect of *tlr5a* deficiency appeared to be specific to flagellated bacterial infections, as demonstrated by the differential response to LPS treatment.

These findings emphasize the critical role of *tlr5a* in orchestrating innate immune responses against bacterial infections, particularly *E. piscicida*. The data underscore the importance of *tlr5a* in regulating various aspects of the host immune system, including the modulation of pro-inflammatory responses, ROS production, and phagocytic cell recruitment. Understanding the intricate interplay between *tlr5a* and bacterial infections can provide valuable insights into the dynamics of host-pathogen interactions. Our results suggest that *tlr5a* is crucial for flagellin recognition and enhancing the adhesion ability of flagellin bacteria, thereby facilitating bacterial invasion. However, the absence of

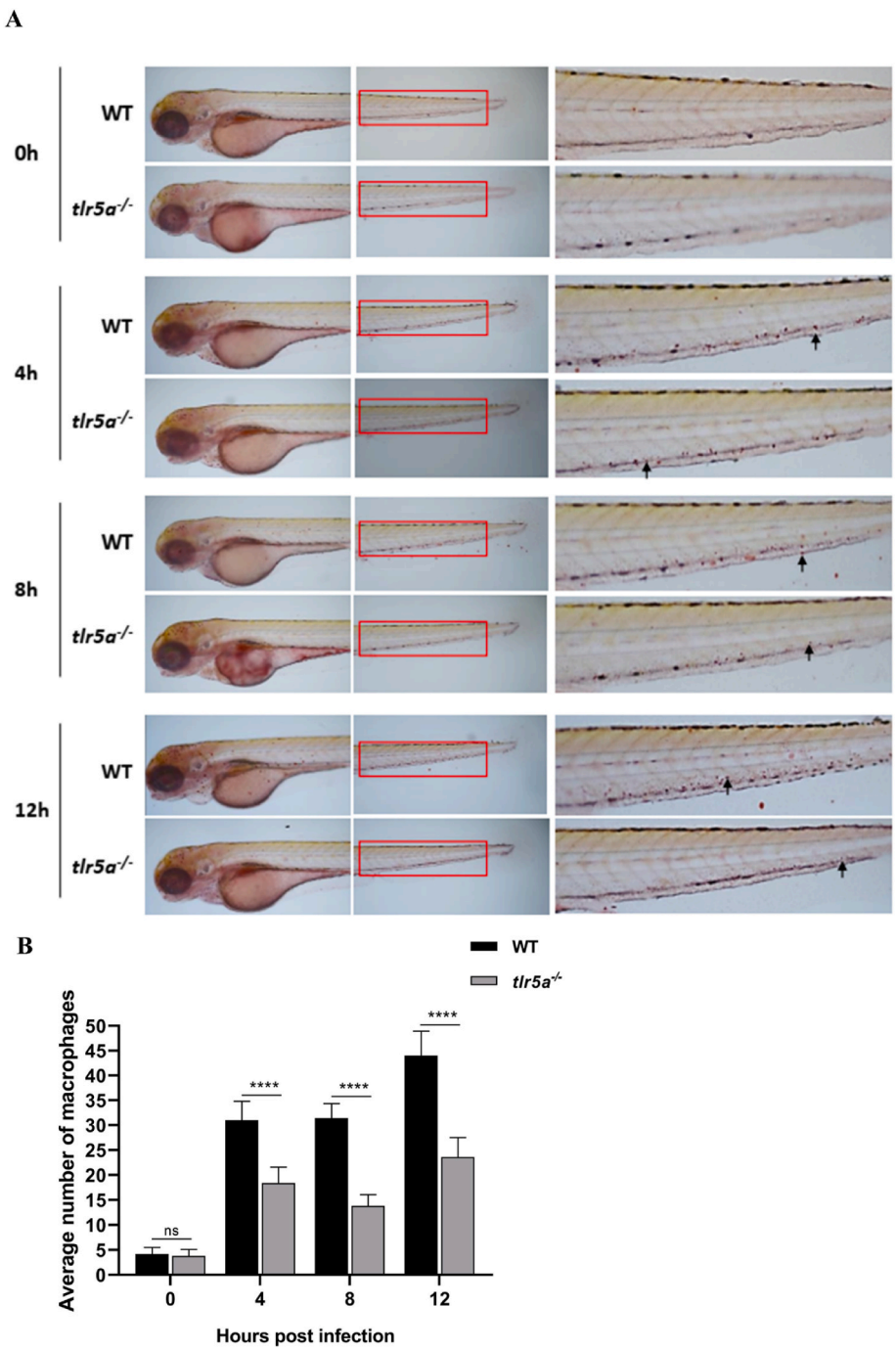


**Fig. 13.** Impact of *tlr5a* deficiency on macrophage production during *E. piscicida* infection. Immersion of 3 dpf WT and *tlr5a*$^{-/-}$ zebrafish larvae in *E. piscicida* was followed by neutral red staining at 0, 4, 8, and 12 hpi to visualize macrophages **(A)**. The resulting average macrophage count was graphed **(B)**. Each bar represents the average macrophage count, with the SD indicated by the error bars (n = 10). Statistical significance between the WT and *tlr5a*$^{-/-}$ fish was determined using Student's *t*-test (ns, non-significance, $p > 0.05$; ****$p \leq 0.0001$).

*tlr5a* might impair infection efficiency while attenuating the over-activation of the immune response against flagellin bacterial infections, subsequently reducing cell damage and apoptosis.

Targeting key immune receptors, such as TLR5a, may alter host–pathogen interactions by reducing bacterial adhesion and inflammatory responses linked to morbidity and mortality in *E. piscicida* infections. Thus, *tlr5a*$^{-/-}$ offers potential avenues for the development of targeted therapeutic strategies against bacterial diseases.

## Ethics statement

This study was performed in line with the standards established by the Animal Experiment Ethics Committee of Jeju National University (approval number: 2019–0014).

## CRediT authorship contribution statement

Each author had been sufficiently involved in the work. Their personal contributions in this work following:

**H.M.S.M. Wijerathna:** Conceptualization, Methodology,

Investigation, Formal analysis Writing - Original Draft. **Sumi Jung:** Methodology, Investigation, Writing - Review & Editing. **Jehee Lee:** Resources, Supervision, Writing - Review & Editing, Project administration, Funding acquisition.

## Funding

This study was supported by the Basic Science Research Program of the National Research Foundation of Korea (NRF), the Ministry of Education (RS-2019-NR040078), the Korea Institute of Marine Science and Technology Promotion (KIMST), and the Ministry of Oceans and Fisheries (RS-2022-KS221670).

## Declaration of competing interest

None of the authors has declared that competing interests exist.

## Acknowledgments

This study was supported by the Basic Science Research Program of the National Research Foundation of Korea (NRF), the Ministry of Education (RS-2019-NR040078), the Korea Institute of Marine Science and Technology Promotion (KIMST), and the Ministry of Oceans and Fisheries (RS-2022-KS221670).

## Data availability

Data will be made available on request.

## References

[1] F. Hayashi, K.D. Smith, A. Ozinsky, T.R. Hawn, E.C. Yi, D.R. Goodlett, J.K. Eng, S. Akira, D.M. Underhill, A. Aderem, The innate immune response to bacterial flagellin is mediated by toll-like receptor 5, Nature 410 (2001) 1099–1103, https://doi.org/10.1038/35074106.

[2] C.G.P. Voogdt, J.A. Wagenaar, J.P.M. Van Putten, Duplicated TLR5 of zebrafish functions as a heterodimeric receptor, Proc. Natl. Acad. Sci. USA 115 (2018), https://doi.org/10.1073/pnas.1719245115.

[3] S. Yoon, O. Kurnasov, V. Natarajan, M. Hong, A.V. Gudkov, A.L. Osterman, I. A. Wilson, Structural basis of TLR5-Flagellin recognition and signaling, Science 335 (2012) 859–864, https://doi.org/10.1126/science.1215584.

[4] I. Caballero, J. Boyd, C. Almiñana, J.A. Sánchez-López, S. Basatvat, M. Montazeri, N. Maslehat Lay, S. Elliott, D.G. Spiller, M.R.H. White, A. Fazeli, Understanding the dynamics of toll-like receptor 5 response to flagellin and its regulation by estradiol, Sci. Rep. 7 (2017) 40981, https://doi.org/10.1038/srep40981.

[5] V.V. Kravchenko, G.F. Kaufmann, Bacterial inhibition of inflammatory responses via TLR-Independent mechanisms: bacterial inhibition of inflammatory responses, Cell. Microbiol. 15 (2013) 527–536, https://doi.org/10.1111/cmi.12109.

[6] J. Gao, M. Liu, H. Guo, K. Zhu, B. Liu, B. Liu, N. Zhang, D. Zhang, ROS induced by Streptococcus agalactiae activate inflammatory responses via the TNF-α/NF-κB signaling pathway in golden pompano Trachinotus ovatus (Linnaeus, 1758), Antioxidants 11 (2022) 1809, https://doi.org/10.3390/antiox11091809.

[7] A.F. Seixas, A.P. Quendera, J.P. Sousa, A.F.Q. Silva, C.M. Arraiano, J.M. Andrade, Bacterial response to oxidative stress and RNA oxidation, Front. Genet. 12 (2022) 821535, https://doi.org/10.3389/fgene.2021.821535.

[8] Z. Liao, C. Yang, R. Jiang, W. Zhu, Y. Zhang, J. Su, Cyprinid-specific duplicated membrane TLR5 senses dsRNA as functional homodimeric receptors, EMBO Rep. 23 (2022) e54281, https://doi.org/10.15252/embr.202154281.

[9] C. Dai, L. Yang, J. Jin, H. Wang, S. Wu, W. Bao, Regulation and molecular mechanism of TLR5 on resistance to Escherichia coli F18 in weaned piglets, Animals 9 (2019) 735, https://doi.org/10.3390/ani9100735.

[10] J. Haiko, B. Westerlund-Wikström, The role of the bacterial flagellum in adhesion and virulence, Biology 2 (2013) 1242–1267, https://doi.org/10.3390/biology2041242.

[11] S. Uematsu, M.H. Jang, N. Chevrier, Z. Guo, Y. Kumagai, M. Yamamoto, H. Kato, N. Sougawa, H. Matsui, H. Kuwata, H. Hemmi, C. Coban, T. Kawai, K.J. Ishii, O. Takeuchi, M. Miyasaka, K. Takeda, S. Akira, Detection of pathogenic intestinal bacteria by toll-like receptor 5 on intestinal CD11c+ lamina propria cells, Nat. Immunol. 7 (2006) 868–874, https://doi.org/10.1038/ni1362.

[12] N. Buján, A. Toranzo, B. Magariños, Edwardsiella piscicida: a significant bacterial pathogen of cultured fish, Dis. Aquat. Org. 131 (2018) 59–71, https://doi.org/10.3354/dao03281.

[13] K.Y. Leung, Q. Wang, Z. Yang, B.A. Siame, *Edwardsiella piscicida* : a versatile emerging pathogen of fish, Virulence 10 (2019) 555–567, https://doi.org/10.1080/21505594.2019.1621648.

[14] S.B. Park, T. Aoki, T.S. Jung, Pathogenesis of and strategies for preventing Edwardsiella tarda infection in fish, Vet. Res. 43 (2012) 67, https://doi.org/10.1186/1297-9716-43-67.

[15] S.-I. Park, H. Wakabayashi, Y. Watanabe, Serotype and virulence of Edwardsiella tarda isolated from eel and their environment, Fish Pathol. 18 (1983) 85–89, https://doi.org/10.3147/jsfp.18.85.

[16] S. Mekasha, D. Linke, Secretion systems in gram-negative bacterial fish pathogens, Front. Microbiol. 12 (2021) 782673, https://doi.org/10.3389/fmicb.2021.782673.

[17] Y. Qian, D. Zhou, M. Li, Y. Zhao, H. Liu, L. Yang, Z. Ying, G. Huang, Application of CRISPR-Cas system in the diagnosis and therapy of ESKAPE infections, Front. Cell. Infect. Microbiol. 13 (2023) 1223696, https://doi.org/10.3389/fcimb.2023.1223696.

[18] P. Singh, S.A. Ali, Impact of CRISPR-Cas9-Based genome engineering in farm animals, Vet. Sci. 8 (2021) 122, https://doi.org/10.3390/vetsci8070122.

[19] B. Bauer, A. Mally, D. Liedtke, Zebrafish embryos and Larvae as alternative animal models for toxicity testing, Indian J. Manag. Sci. 22 (2021) 13417, https://doi.org/10.3390/ijms222413417.

[20] Y. Li, Z. Jia, S. Zhang, X. He, Progress in gene-editing technology of zebrafish, Biomolecules 11 (2021) 1300, https://doi.org/10.3390/biom11091300.

[21] K. Howe, M.D. Clark, C.F. Torroja, J. Torrance, C. Berthelot, M. Muffato, J. E. Collins, S. Humphray, K. McLaren, L. Matthews, S. McLaren, I. Sealy, M. Caccamo, C. Churcher, C. Scott, J.C. Barrett, R. Koch, G.-J. Rauch, S. White, W. Chow, B. Kilian, L.T. Quintais, J.A. Guerra-Assunção, Y. Zhou, Y. Gu, J. Yen, J.-H. Vogel, T. Eyre, S. Redmond, R. Banerjee, J. Chi, B. Fu, E. Langley, S.F. Maguire, G.K. Laird, D. Lloyd, E. Kenyon, S. Donaldson, H. Sehra, J. Almeida-King, J. Loveland, S. Trevanion, M. Jones, M. Quail, D. Willey, A. Hunt, J. Burton, S. Sims, K. McLay, B. Plumb, J. Davis, C. Clee, K. Oliver, R. Clark, C. Riddle, D. Elliott, G. Threadgold, G. Harden, D. Ware, S. Begum, B. Mortimore, G. Kerry, P. Heath, B. Phillimore, A. Tracey, N. Corby, M. Dunn, C. Johnson, J. Wood, S. Clark, S. Pelan, G. Griffiths, M. Smith, R. Glithero, P. Howden, N. Barker, C. Lloyd, C. Stevens, J. Harley, K. Holt, G. Panagiotidis, J. Lovell, H. Beasley, C. Henderson, D. Gordon, K. Auger, D. Wright, J. Collins, C. Raisen, L. Dyer, K. Leung, L. Robertson, K. Ambridge, D. Leongamornlert, S. McGuire, R. Gilderthorp, C. Griffiths, D. Manthravadi, S. Nichol, G. Barker, S. Whitehead, M. Kay, J. Brown, C. Murnane, E. Gray, M. Humphries, N. Sycamore, D. Barker, D. Saunders, J. Wallis, A. Babbage, S. Hammond, M. Mashreghi-Mohammadi, L. Barr, S. Martin, P. Wray, A. Ellington, N. Matthews, M. Ellwood, R. Woodmansey, G. Clark, J.D. Cooper, A. Tromans, D. Grafham, C. Skuce, R. Pandian, R. Andrews, E. Harrison, A. Kimberley, J. Garnett, N. Fosker, R. Hall, P. Garner, D. Kelly, C. Bird, S. Palmer, I. Gehring, A. Berger, C.M. Dooley, Z. Ersan-Ürün, C. Eser, H. Geiger, M. Geisler, L. Karotki, A. Kirn, J. Konantz, M. Konantz, M. Oberländer, S. Rudolph-Geiger, M. Teucke, C. Lanz, G. Raddatz, K. Osoegawa, B. Zhu, A. Rapp, S. Widaa, C. Langford, F. Yang, S.C. Schuster, N.P. Carter, J. Harrow, Z. Ning, J. Herrero, S.M.J. Searle, A. Enright, R. Geisler, R.H.A. Plasterk, C. Lee, M. Westerfield, P.J. De Jong, L.I. Zon, J.H. Postlethwait, C. Nüsslein-Volhard, T.J.P. Hubbard, H.R. Crollius, J. Rogers, D.L. Stemple, The zebrafish reference genome sequence and its relationship to the human genome, Nature 496 (2013) 498–503, https://doi.org/10.1038/nature12111.

[22] A. Avdesh, M. Chen, M.T. Martin-Iverson, A. Mondal, D. Ong, S. Rainey-Smith, K. Taddei, M. Lardelli, D.M. Groth, G. Verdile, R.N. Martins, Regular care and maintenance of a zebrafish (Danio rerio) laboratory: an introduction, JoVE J. (2012) 4196, https://doi.org/10.3791/4196.

[23] T. Hubbard, The Ensembl genome database project, Nucleic Acids Res. 30 (2002) 38–41, https://doi.org/10.1093/nar/30.1.38.

[24] D. Benson, D.J. Lipman, J. Ostell, GenBank, Nucleic Acids Res. 21 (1993) 2963–2965, https://doi.org/10.1093/nar/21.13.2963.

[25] F. Sievers, D.G. Higgins, The clustal omega multiple alignment package, in: K. Katoh (Ed.), Multiple Sequence Alignment, Springer US, New York, NY, 2021, pp. 3–16, https://doi.org/10.1007/978-1-0716-1036-7_1.

[26] P. Rice, I. Longden, A. Bleasby, EMBOSS: the European molecular biology open software suite, Trends Genet. 16 (2000) 276–277, https://doi.org/10.1016/S0168-9525(00)02024-2.

[27] K. Tamura, G. Stecher, S. Kumar, MEGA11: molecular evolutionary genetics analysis version 11, Mol. Biol. Evol. 38 (2021) 3022–3027, https://doi.org/10.1093/molbev/msab120.

[28] L.-E. Jao, S.R. Wente, W. Chen, Efficient multiplex biallelic zebrafish genome editing using a CRISPR nuclease system, Proc. Natl. Acad. Sci. USA 110 (2013) 13904–13909, https://doi.org/10.1073/pnas.1308335110.

[29] G.K. Varshney, W. Pei, M.C. LaFave, J. Idol, L. Xu, V. Gallardo, B. Carrington, K. Bishop, M. Jones, M. Li, U. Harper, S.C. Huang, A. Prakash, W. Chen, R. Sood, J. Ledin, S.M. Burgess, High-throughput gene targeting and phenotyping in zebrafish using CRISPR/Cas9, Genome Res. 25 (2015) 1030–1042, https://doi.org/10.1101/gr.186379.114.

[30] H.J. Kim, H.J. Lee, H. Kim, S.W. Cho, J.-S. Kim, Targeted genome editing in human cells with zinc finger nucleases constructed via modular assembly, Genome Res. 19 (2009) 1279–1288, https://doi.org/10.1101/gr.089417.108.

[31] H.M.S.M. Wijerathna, K.A.S.N. Shanaka, S.S. Raguvaran, B.P.M.V. Jayamali, S.-H. Kim, M.-J. Kim, S. Jung, J. Lee, CRISPR/Cas9-Mediated fech knockout zebrafish: unraveling the pathogenesis of erythropoietic protoporphyria and facilitating drug screening, Indian J. Manag. Sci. 25 (2024) 10819, https://doi.org/10.3390/ijms251910819.

[32] A. Soorni, M. Rezvani, H. Bigdeli, Transcriptome-guided selection of stable reference genes for expression analysis in spinach, Sci. Rep. 14 (2024) 22113, https://doi.org/10.1038/s41598-024-73444-2.

[33] K. Shekh, S. Tang, S. Niyogi, M. Hecker, Expression stability and selection of optimal reference genes for gene expression normalization in early life stage

rainbow trout exposed to cadmium and copper, Aquat. Toxicol. 190 (2017) 217–227, https://doi.org/10.1016/j.aquatox.2017.07.009.
[34] L. Hou, H. Zhu, W. Xian, Y. Ma, Selection and validation of stable reference genes in potato infected by Pectobacterium atrosepticum using real-time quantitative PCR, Sci. Rep. 15 (2025) 14205, https://doi.org/10.1038/s41598-025-97542-x.
[35] M.E. Pressley, P.E. Phelan, P. Eckhard Witten, M.T. Mellon, C.H. Kim, Pathogenesis and inflammatory response to Edwardsiella tarda infection in the zebrafish, Dev. Comp. Immunol. 29 (2005) 501–513, https://doi.org/10.1016/j.dci.2004.10.007.
[36] T. Zhang, C. Zhang, J. Zhang, J. Lin, D. Song, P. Zhang, Y. Liu, L. Chen, L. Zhang, Cadmium impairs zebrafish swim bladder development via ROS mediated inhibition of the Wnt/Hedgehog pathway, Aquat. Toxicol. 247 (2022) 106180, https://doi.org/10.1016/j.aquatox.2022.106180.
[37] R. Chaiprasongsuk, P. Achararit, P. Jarutatsanangkoon, P. Nonthasaen, W. Mahikul, A. Chaiprasongsuk, U. Panich, P. Prombut, Quantitative analysis of the 2D tissue skin layer with fluorescent dyes, in: 2022 19th International Joint Conference on Computer Science and Software Engineering (JCSSE), IEEE, Bangkok, Thailand, 2022, pp. 1–6, https://doi.org/10.1109/JCSSE54890.2022.9836243.
[38] S. Wu, L. Wang, J. Li, G. Xu, M. He, Y. Li, R. Huang, Salmonella spv locus suppresses host innate immune responses to bacterial infection, Fish Shellfish Immunol. 58 (2016) 387–396, https://doi.org/10.1016/j.fsi.2016.09.042.
[39] S. Verma, R. Sowdhamini, A genome-wide search of Toll/Interleukin-1 receptor (TIR) domain-containing adapter molecule (TICAM) and their evolutionary divergence from other TIR domain containing proteins, Biol. Direct 17 (2022) 24, https://doi.org/10.1186/s13062-022-00335-9.
[40] M. Westerfield, THE ZEBRAFISH BOOK, A Guide for the Laboratory Use of Zebrafish (Danio rerio), fourth ed., University of Oregon, Eugene, 2000. https://zfin.org/zf_info/zfbook/zfbk.html.
[41] D.A. Kane, C.B. Kimmel, The zebrafish midblastula transition, Development 119 (1993) 447–456, https://doi.org/10.1242/dev.119.2.447.
[42] D. Autran, C. Baroux, M.T. Raissig, T. Lenormand, M. Wittig, S. Grob, A. Steimer, M. Barann, U.C. Klostermeier, O. Leblanc, J.-P. Vielle-Calzada, P. Rosenstiel, D. Grimanelli, U. Grossniklaus, Maternal epigenetic pathways control parental contributions to arabidopsis early embryogenesis, Cell 145 (2011) 707–719, https://doi.org/10.1016/j.cell.2011.04.014.
[43] Y. Cao, E. Zhang, J. Yang, Y. Yang, J. Yu, Y. Xiao, W. Li, D. Zhou, Y. Li, B. Zhao, H. Yan, M. Lu, M. Zhong, H. Yan, Frontline science: Nasal epithelial GM-CSF contributes to TLR5-mediated modulation of airway dendritic cells and subsequent IgA response, J. Leukoc. Biol. 102 (2017) 575–587, https://doi.org/10.1189/jlb.3HI0816-368RR.
[44] R. Wang, J. Ahmed, G. Wang, I. Hassan, Y. Strulovici-Barel, J. Salit, J.G. Mezey, R. G. Crystal, Airway epithelial expression of TLR5 is downregulated in healthy smokers and smokers with chronic obstructive pulmonary disease, J. Immunol. 189 (2012) 2217–2225, https://doi.org/10.4049/jimmunol.1101895.
[45] A. Tiron, C. Vasilescu, [Role of the spleen in immunity. Immunologic consequences of splenectomy], Chirurgia (Bucur) 103 (2008) 255–263.
[46] V. Racanelli, B. Rehermann, The liver as an immunological organ, Hepatology 43 (2006) S54–S62, https://doi.org/10.1002/hep.21060.
[47] M.W. Robinson, C. Harmon, C. O'Farrelly, Liver immunology and its role in inflammation and homeostasis, Cell. Mol. Immunol. 13 (2016) 267–276, https://doi.org/10.1038/cmi.2016.3.
[48] X. Liu, H. Wu, X. Chang, Y. Tang, Q. Liu, Y. Zhang, Notable mucosal immune responses induced in the intestine of zebrafish (Danio rerio) bath-vaccinated with a live attenuated Vibrio anguillarum vaccine, Fish Shellfish Immunol. 40 (2014) 99–108, https://doi.org/10.1016/j.fsi.2014.06.030.
[49] F. Zhan, Y. Li, F. Shi, Z. Lu, M. Yang, Q. Li, L. Lin, Z. Qin, Characterization analysis of TLR5a and TLR5b immune response after different bacterial infection in grass carp (Ctenopharyngodon idella), Fish Shellfish Immunol. 136 (2023) 108716, https://doi.org/10.1016/j.fsi.2023.108716.
[50] J. Yang, H. Yan, TLR5: beyond the recognition of flagellin, Cell. Mol. Immunol. 14 (2017) 1017–1019, https://doi.org/10.1038/cmi.2017.122.
[51] L.R. Lopetuso, R. Jia, X.-M. Wang, L.-G. Jia, V. Petito, W.A. Goodman, J. B. Meddings, F. Cominelli, B.K. Reuter, T.T. Pizarro, Epithelial-specific toll-like receptor (TLR)5 activation mediates barrier dysfunction in experimental ileitis, Inflamm. Bowel Dis. 23 (2017) 392–403, https://doi.org/10.1097/MIB.0000000000001035.
[52] B. Chassaing, R.E. Ley, A.T. Gewirtz, Intestinal epithelial cell toll-like receptor 5 regulates the intestinal microbiota to prevent low-grade inflammation and metabolic syndrome in mice, Gastroenterology 147 (2014) 1363–1377.e17, https://doi.org/10.1053/j.gastro.2014.08.033.
[53] J. Wu, Z. Meng, M. Jiang, E. Zhang, M. Trippler, R. Broering, A. Bucchi, F. Krux, U. Dittmer, D. Yang, M. Roggendorf, G. Gerken, M. Lu, J.F. Schlaak, Toll-like receptor-induced innate immune responses in non-parenchymal liver cells are cell type-specific, Immunology 129 (2010) 363–374, https://doi.org/10.1111/j.1365-2567.2009.03179.x.
[54] A.T. Gewirtz, T.A. Navas, S. Lyons, P.J. Godowski, J.L. Madara, Cutting edge: bacterial flagellin activates basolaterally expressed TLR5 to induce epithelial proinflammatory gene expression, J. Immunol. 167 (2001) 1882–1885, https://doi.org/10.4049/jimmunol.167.4.1882.
[55] T. Tallant, A. Deb, N. Kar, J. Lupica, M.J. De Veer, J.A. DiDonato, Flagellin acting via TLR5 is the major activator of key signaling pathways leading to NF-κB and proinflammatory gene program activation in intestinal epithelial cells, BMC Microbiol. 4 (2004) 33, https://doi.org/10.1186/1471-2180-4-33.
[56] Z. Sui, H. Xu, H. Wang, S. Jiang, H. Chi, L. Sun, Intracellular trafficking pathways of Edwardsiella tarda: from Clathrin- and Caveolin-mediated endocytosis to endosome and lysosome, Front. Cell. Infect. Microbiol. 7 (2017) 400, https://doi.org/10.3389/fcimb.2017.00400.
[57] H.-S. Hwang, J.-W. Kim, S.-H. Oh, J.H. Song, J.-W. Yang, Y. Zang, Y.-H. Kim, S.-E. Lee, Y.-C. Hwang, J.-T. Koh, TLR5 activation induces expression of the pro-inflammatory mediator Urokinase Plasminogen activator via NF-κB and MAPK signalling pathways in human dental pulp cells, Int. Endod. J. 52 (2019) 1479–1488, https://doi.org/10.1111/iej.13140.
[58] G. Weng, U.S. Bhalla, R. Iyengar, Complexity in biological signaling systems, Science 284 (1999) 92–96, https://doi.org/10.1126/science.284.5411.92.
[59] M. Boutros, H. Agaisse, N. Perrimon, Sequential activation of signaling pathways during innate immune responses in drosophila, Dev. Cell 3 (2002) 711–722, https://doi.org/10.1016/S1534-5807(02)00325-8.
[60] B. Beutler, E.Th Rietschel, Innate immune sensing and its roots: the story of endotoxin, Nat. Rev. Immunol. 3 (2003) 169–176, https://doi.org/10.1038/nri1004.
[61] C.R.H. Raetz, C. Whitfield, Lipopolysaccharide endotoxins, Annu. Rev. Biochem. 71 (2002) 635–700, https://doi.org/10.1146/annurev.biochem.71.110601.135414.
[62] S.I. Miller, R.K. Ernst, M.W. Bader, LPS, TLR4 and infectious disease diversity, Nat. Rev. Microbiol. 3 (2005) 36–46, https://doi.org/10.1038/nrmicro1068.
[63] A. Poltorak, X. He, I. Smirnova, M.-Y. Liu, C.V. Huffel, X. Du, D. Birdwell, E. Alejos, M. Silva, C. Galanos, M. Freudenberg, P. Ricciardi-Castagnoli, B. Layton, B. Beutler, Defective LPS signaling in C3H/HeJ and C57BL/10ScCr mice: mutations in *Tlr4* gene, Science 282 (1998) 2085–2088, https://doi.org/10.1126/science.282.5396.2085.
[64] D.V. Grebennikova, U.K. Shandilya, N.A. Karrow, Beyond TLR4 and its alternative lipopolysaccharide (LPS) sensing pathways in zebrafish, Genes 16 (2025) 1014, https://doi.org/10.3390/genes16091014.
[65] V. Feuillet, S. Medjane, I. Mondor, O. Demaria, P.P. Pagni, J.E. Galán, R.A. Flavell, L. Alexopoulou, Involvement of toll-like receptor 5 in the recognition of flagellated bacteria, Proc. Natl. Acad. Sci. USA 103 (2006) 12487–12492, https://doi.org/10.1073/pnas.0605200103.
[66] R. Spooner, Ö. Yilmaz, The role of reactive-oxygen-species in microbial persistence and inflammation, Indian J. Manag. Sci. 12 (2011) 334–352, https://doi.org/10.3390/ijms12010334.
[67] M.L. Circu, T.Y. Aw, Reactive oxygen species, cellular redox systems, and apoptosis, Free Radic. Biol. Med. 48 (2010) 749–762, https://doi.org/10.1016/j.freeradbiomed.2009.12.022.
[68] J.-H. Joo, J.-H. Ryu, C.-H. Kim, H.J. Kim, M.-S. Suh, J.-O. Kim, S.Y. Chung, S. N. Lee, H.M. Kim, Y.S. Bae, J.-H. Yoon, Dual oxidase 2 is essential for the toll-like receptor 5-Mediated inflammatory response in airway mucosa, Antioxidants Redox Signal. 16 (2012) 57–70, https://doi.org/10.1089/ars.2011.3898.
[69] E.A. Harvie, A. Huttenlocher, Neutrophils in host defense: new insights from zebrafish, J. Leukoc. Biol. 98 (2015) 523–537, https://doi.org/10.1189/jlb.4MR1114-524R.
[70] N. Borregaard, Neutrophils, from marrow to microbes, Immunity 33 (2010) 657–670, https://doi.org/10.1016/j.immuni.2010.11.011.
[71] C. Nathan, Neutrophils and immunity: challenges and opportunities, Nat. Rev. Immunol. 6 (2006) 173–182, https://doi.org/10.1038/nri1785.
[72] X. Zhang, Y. Zhao, Q. Wu, J. Lin, R. Fang, W. Bi, G. Dong, J. Li, Y. Zhang, J. Cao, T. Zhou, Zebrafish and galleria mellonella: models to identify the subsequent infection and evaluate the immunological differences in different Klebsiella pneumoniae intestinal colonization strains, Front. Microbiol. 10 (2019) 2750, https://doi.org/10.3389/fmicb.2019.02750.
[73] V. Torraca, S. Masud, H.P. Spaink, A.H. Meijer, Macrophage-pathogen interactions in infectious diseases: new therapeutic insights from the zebrafish host model, Dis. Model. Mech. 7 (2014) 785–797, https://doi.org/10.1242/dmm.015594.
[74] A. Aderem, Phagocytosis and the inflammatory response, J. Infect. Dis. 187 (2003) S340–S345, https://doi.org/10.1086/374747.
[75] C. Murdoch, A. Giannoudis, C.E. Lewis, Mechanisms regulating the recruitment of macrophages into hypoxic areas of tumors and other ischemic tissues, Blood 104 (2004) 2224–2234, https://doi.org/10.1182/blood-2004-03-1109.
[76] G. Arango Duque, A. Descoteaux, Macrophage cytokines: involvement in immunity and infectious diseases, Front. Immunol. 5 (2014), https://doi.org/10.3389/fimmu.2014.00491.